*This work is supported in part through funds provided by the Atomic Energy Commission under Contract No. AT(11-1)-3069 and the National Science Foundation under Grant Nos. NSF GP 29705 and NSF GP 32998X.

†Permanent address: Dept. of Physics, University of Massachusetts at Boston, Boston, Mass. 02116.

[1]J. Sandweiss, J. Sunderland, W. Turner, W. Willis, and L. Keller, Phys. Rev. Lett. 30, 1002 (1973).

[2]A. L. Sessoms, H. H. Williams, W. W. Sapp, R. C. Larsen, L. W. Smith, L. B. Leipuner, H. Kasha, R. K. Adair, R. Turner, Bull. Am. Phys. Soc. 18, 615 (1973); S. Merlan, H. Kasha, P. J. Wanderer, R. K. Adair, C. M. Ankenbrandt, R. C. Larsen, L. B. Leipuner, L. W. Smith, R. Stefanski, F. T. Shively, Phys. Rev. D (to be published).

[3]A general theoretical and experimental review, containing definitions and explanations of the parameters used in K_{l3} decays, has been published by L.-M. Chounet, J.-M. Gaillard, and M. K. Gaillard, Phys. Rep. 4C, 199 (1972).

[4]N. Cabibbo and A. Maksymowicz, Phys. Lett. 9, 352 (1964); 11, 360(E) (1964); 14, 72(E) (1965).

[5]N. Byers, S. W. MacDowell, and C. N. Yang, in *Proceedings of the International Seminar on High Energy Physics and Elementary Particles, Trieste, 1965* (International Atomic Energy Agency, Vienna, 1965) p. 953.

[6]E. S. Ginsberg, Phys. Rev. D 4, 2893 (1971).

[7]J. D. Bjorken, Phys. Rev. 148, 1467 (1967).

[8]K. Johnson, F. E. Low, and H. Suura, Phys. Rev. Lett. 18, 1224 (1967).

[9]N. Cabibbo, L. Maiani, and G. Preparata, Phys. Lett. 25B, 31 (1967); 25B, 132 (1967).

[10]A. Sirlin, Phys. Rev. Lett. 19, 877 (1967).

[11]E. S. Abers, R. E. Norton, D. A. Dicus, and H. Quinn, Phys. Rev. 167, 1461 (1968).

[12]G. Preparata and W. I. Weisberger, Phys. Rev. 175, 1965 (1968).

[13]References to work on the development of these theories are cited by B. W. Lee, in *Proceedings of the XVI International Conference on High Energy Physics, Chicago-Batavia, Ill., 1972,* edited by J. D. Jackson and A. Roberts (NAL, Batavia, Ill., 1973).

[14]E. S. Ginsberg, Phys. Rev. 171, 1675 (1968); 174, 2169(E) (1968); 187, 2280(E) (1969), in particular Eqs. (1), (2), (6), (14), and (15).

[15]We conform to the metric and representation of the γ matrices used by S. Schweber, *An Introduction to Relativistic Quantum Field Theory* (Harper and Row, New York, 1961).

[16]E. S. Ginsberg, Phys. Rev. D 1, 229 (1970). Note: The factors of $\frac{1}{2}$ multiplying the dilogarithms in the second line of Eq. (20) are copying errors and should be omitted. The numerical results are not significantly changed (generally by 0.0 to 0.3% in the Dalitz plot). A corrected version of Fig. 2(a) is given in Fig. 1 of this paper.

[17]Infrared-divergent terms, which cancel exactly when all the contributions to the radiative corrections are added, have been omitted.

[18]E. S. Ginsberg, Phys. Rev. 162, 1570 (1967); 187, 2280(E) (1969).

PHYSICAL REVIEW D VOLUME 8, NUMBER 11 1 DECEMBER 1973

Partial-Wave Analysis of the Deck Amplitude for $\pi N \to \pi\pi\pi N$ *†

G. Ascoli, L. M. Jones,
B. Weinstein, and H. W. Wyld, Jr.
Physics Department, University of Illinois at Urbana-Champaign, Urbana, Illinois 61801

(Received 6 August 1973)

We present a straightforward method for calculating the amplitudes of the various *JMLS* states in the final 3π system of the reaction $\pi N \to \pi\pi\pi N$, assuming a Deck-model form for the production process. This calculation allows us to study relative phases of different partial waves, and the nucleon spin structure of the production amplitudes, in an unambiguous fashion. We find that the magnitudes and phases of 3π partial waves obtained by this method agree reasonably well with those obtained by applying an experimental fitting program to Monte Carlo events generated using the Deck formula; this may be interpreted as a check on the assumptions of the fitting program. Likewise, the magnitudes and phases agree reasonably well with those obtained from the data, confirming the belief that the A_1 and A_3 effects are probably produced by the Deck mechanism. In the rest system of the three pions, only one nucleon helicity-amplitude combination is dominant. The method of analysis can be applied to similar models for other production reactions.

I. INTRODUCTION

Considerable interest in the A_1 "resonance" has been generated by partial-wave fits to the data for the reaction[1-3]

$$\pi^- p \to \pi^-\pi^+\pi^- p . \tag{1.1}$$

These have demonstrated that the A_1 effect occurs in the $J^P = 1^+$, $L = 0$ $\rho\pi$ system, but that the phase of the amplitude changes very slowly as $m_{\rho\pi}$ in-

creases through the A_1 mass. This is to be contrasted with the rapid variation of phase expected for a true resonant state described by a Breit-Wigner formula. In an associated article, hereafter referred to as II,[4] we show that Monte Carlo events generated by a computer according to a generalized Deck model resemble the data in many particulars. When partial-wave amplitudes are extracted by fitting the Monte Carlo events with the same program used to fit the experimental data, the magnitudes and phases in the 1^+ system (and in several other partial waves) are quite similar to the data. This leads us to conclude (in II) that the effects embodied in the Reggeized Deck model provide the basic framework for nonresonant dynamics of the 3π system.

In II we depend on the program FIT developed by Ascoli *et al.*[1-3] to perform the partial-wave analysis. This program operates on data, i.e., actual or Monte Carlo generated events distributed according to bilinear combinations of amplitudes. The data are fitted, using the maximum-likelihood method, to certain formulas assumed to describe the reaction $\pi^- p \to \pi^-\pi^+\pi^- p$. These formulas are not completely general, so it is necessary to understand and keep in mind the assumptions made by FIT. This is particularly so for events generated according to the Deck model, since the mechanism assumed in that model is somewhat contrary to the mechanism assumed in the formulas used by FIT. Furthermore, in dealing with a theoretical model such as the Deck model the amplitude itself is directly available, so that it is clearly awkward and unnecessary to extract the partial-wave amplitudes from the bilinear combinations of them which describe the distributions of events.

In the present paper we therefore carry through a direct partial-wave analysis of the Deck amplitude, independently of the FIT program. The partial-wave analysis is achieved by multiplying the Deck amplitude by a suitable angular momentum function and integrating over appropriate angular variables. The theoretical formulas for this direct angular momentum analysis are developed in Sec. II. The results of numerical evaluation of the formulas are given in Sec. III. From these results we can obtain some understanding of the physical content of the Deck model as represented by its angular momentum decomposition, independent of any assumptions of the FIT program. In Sec. IV of the paper the direct partial-wave analysis of Secs. II and III is compared with an angular momentum analysis by FIT of Monte Carlo events generated according to the same Deck model. This comparison enables us to make some assessment of the limitations of FIT, at least as applied to Deck-like models.

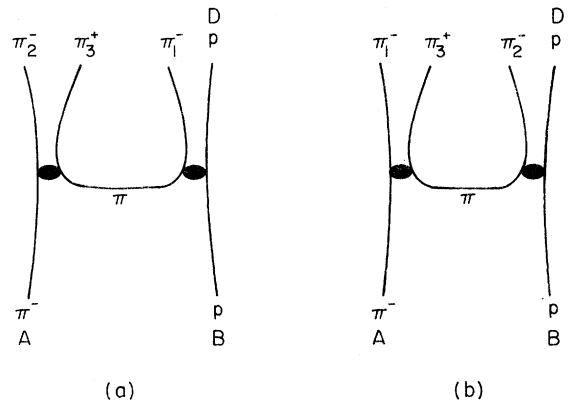

FIG. 1. The two amplitudes considered in this paper. Each has a $\pi^+\pi^-$ scattering amplitude and a $\pi^- p$ elastic amplitude connected by a Reggeized pion propagator.

In Sec. V of the paper we present a detailed discussion of symmetry properties with particular reference to the helicity structure of our results. Some comments in summary are given in Sec. VI.

The Deck model employed in this paper is similar in all regards save one to the Deck model employed in II. Here we discuss the two-diagram model illustrated in Fig. 1. The two contributions to the amplitude correspond to interchange of the two π^- mesons and thus ensure Bose symmetry. The partial-wave analysis is performed on one of the diagrams [Fig. 1(a)], using angular momentum states referring to the spin S of the $\pi_2^-\ \pi_3^+$ dipion and the orbital angular momentum L of this dipion relative to the other pion π_1^-. Before computing probability distributions the partial-wave series must be summed and the contributions of the second diagram [Fig. 1(b)] obtained by interchanging the two π^- mesons must be added. (This is discussed at some length in Sec. II B.)

The Deck model amplitude corresponding to each of the diagrams of Fig. 1 is the product of three factors: (a) $\pi\pi$ scattering amplitude, (b) Reggeized pion propagator, and (c) πN scattering amplitude. We summarize here the salient features of each:

(a) For the $\pi\pi$ scattering, we use below 1.48 GeV the results from recent phase-shift analyses.[5,6] Since the maximum *three*-pion energy W considered is only 1.9 GeV and since the $\pi\pi$ partial-wave invariant scattering amplitudes change very slowly in the neighborhood of 1.48 GeV, we set these amplitudes equal to their value at 1.48 GeV for energies greater than this value.

For the diagrams in Fig. 1 one of the initial pions for the $\pi\pi$ scattering is off-shell. In our calculation on-shell $\pi\pi$ amplitudes are used, evaluated at the energy and scattering angle determined by the off-shell kinematics. Note also that the $\pi\pi$

amplitudes are on-shell with respect to the spin of the exchanged pion although we use a Reggeized pion propagator.

(b) The Reggeized pion propagator employed is

$$\frac{1}{m_\pi^2 - t_R} e^{-i\pi\alpha(t_R)/2}\left(\frac{s'-u'}{2s_0}\right)^{\alpha(t_R)}, \qquad \alpha(t_R) = t_R - m_\pi^2, \quad s_0 = 1\ \text{GeV}^2. \tag{1.2}$$

For $\alpha = 0$ this reduces to the standard Feynman propagator for a spinless particle. The quantities s' and u' in this formula are calculated for the two-body kinematics indicated in Fig. 2: The dipion $\pi_2^-\pi_3^+$ [corresponding to Fig. 1(a)] is treated as a particle, as is the object (Pomeranchon plus$\cdots$) exchanged at the pp vertex. Thus we use

$$\tfrac{1}{2}(s'-u') = W^2 - m_\pi^2 + \tfrac{1}{2}(t_R - t - s_1), \tag{1.3}$$

where $s_1 = (p_2+p_3)^2 = (\text{dipion mass})^2$ and $W^2 = (p_1+p_2+p_3)^2 = (3\text{-pion mass})^2$. Some reasons for this choice are discussed in II.

By and large we must admit that (1.2) and (1.3) are quite arbitrary, especially since we use these Regge formulas for small $s' = W^2 \gtrsim 1.0\ \text{GeV}^2$. We note, however, that the Regge phase factor in (1.2) is crucial. The relative success of this model in explaining phases obtained in the analysis of experimental data is due to this Regge phase factor; the other phase factor coming from πN scattering provides only small corrections to what one would obtain with a purely real pion propagator and a pure Pomeranchon exchange for the πN scattering. Finally we note that although the Reggeized exchanged pion has spin $\alpha(t)$, the couplings at both ends are those of a spin-zero pion, i.e., only helicity zero is coupled.

(c) For the πN scattering amplitude we again use on-shell amplitudes calculated at the energy and scattering angle determined by the off-shell kinematics. For $E_{\pi N} \leq 2.0$ GeV these amplitudes are calculated from the CERN Theoretical (1967)[7] phase shifts. For $E_{\pi N} \geq 2.2$ GeV we use the Barger-Phillips[8] Regge fit to high-energy πN scattering. In order to achieve continuity in the intermediate region 2.0 GeV $\leq E_{\pi N} \leq 2.2$ GeV we linearly interpolate between the amplitudes calculated from the phase shifts at $E_{\pi N} = 2.0$ GeV and those calculated from the Barger-Phillips formulas at $E_{\pi N} = 2.2$ GeV. In this connection it is worth noting two things: First, high-energy πN scattering satisfies approximate s-channel helicity conservation.[9] Second, although there is a noticeable discontinuity in the πN $\mathcal{A}$ and $\mathcal{B}$ amplitudes as one compares the amplitudes calculated from phase shifts to those calculated from the Barger-Phillips formulas in the intermediate energy region, the discontinuity is much smaller for the dominant s-channel helicity-conserving amplitude.

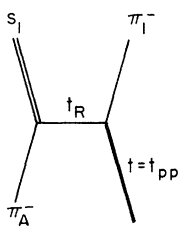

FIG. 2. Kinematics leading to the 3π final state.

A more complicated three-diagram model is discussed in paper II. In addition to the two diagrams of Fig. 1 a third diagram involving $\pi^-\pi^-$ scattering and $\pi^+ p$ scattering is included. This diagram could be partial-wave-analyzed using the methods of this paper, but it would involve an additional recoupling calculation in which SL states referring to the pairing $(\pi_1^-\pi_2^-)\pi_3^+$ are reexpressed in terms of SL states for the pairing $(\pi_2^-\pi_3^+)\pi_1^-$. This is possible but probably difficult for the Deck model, since it would necessitate calculating in detail a small but non-negligible tail of high-L states. In any event we have left out the third diagram in this paper. Since the contribution from $\pi^-\pi^-$ scattering is relatively small, this omission should not seriously detract from the utility of our results. Some measure of the influence of the $\pi^-\pi^-$ scattering events may be obtained by comparing the results presented in Secs. III and IV of this paper with those of paper II.

The calculations presented in this paper are similar in spirit to those of Froggatt and Ranft[10] and Ranft.[11] We have tried to be as realistic as possible with regard to the $\pi\pi$ and πN scattering, whereas Ranft and Froggatt introduce ρ and ϵ mesons treated as particles and use a simplified estimate for the πN scattering. These improvements enable us to calculate the complete Bose-symmetrized amplitudes and distributions in all possible kinematic variables (many of these distributions are given in II). Because we treat all partial waves in $\pi\pi$ scattering on the same footing we are able to calculate the relative phases of amplitudes with different S and to examine the A_3 region as well as the A_1 region.

II. THEORETICAL FORMULAS

A. Partial-Wave Amplitudes

We wish to write down a partial-wave decomposition of the matrix element T for the reaction (1.1). This will be a summation $T = \sum_{JMP} T_{JMP}$ over the contributions in which the three-pion system on the right side of (1.1) has quantum numbers J = total angular momentum, $M = z$ projection of angular momentum, P = parity. In order to write

down an explicit formula for T_{JMP} we work in the center-of-mass system of coordinates for the three pions with the z axis along the direction of motion of the incoming pion as viewed in this system.

The three-pion states can be described in the Dalitz terminology of a pion 1 plus a dipion 23 [Fig. 1(a)]. We take particle 3 to be the π^+, particles 1 and 2 to be the π^-'s. The Bose symmetry will be taken account of by symmetrizing $1 \rightleftarrows 2$ [Fig. 1(b)]. We can use as variables the mass of the dipion $m_{23} = \sqrt{s_1}$ and two sets of polar and azimuthal angles. The four angles necessary are illustrated in Fig. 3; $\Omega_1 = (\theta_1, \varphi_1)$ are the polar and azimuthal angles locating the dipion 23 in the three-pion center-of-mass system, $\overline{\Omega} = (\overline{\theta}_1, \overline{\varphi}_1)$ are the polar and azimuthal angles locating pion 3, the π^+, in the dipion center-of-mass system relative to the same set of axes. An appropriate complete set of angular momentum states for the three-pion system is the set of functions

$$Z_{LS}^{JM}(\Omega_1, \overline{\Omega}_1) = \sum_{M_L, M_S} \langle JM | LSM_L M_S \rangle Y_L^{M_L}(\Omega_1) Y_S^{M_S}(\overline{\Omega}_1) . \tag{2.1}$$

Here S is the angular momentum of the dipion 23 and L is the orbital angular momentum of the dipion relative to the other pion 1. The spherical harmonics are coupled with a Clebsch-Gordan coefficient $\langle JM | LSM_L M_S \rangle$ to obtain a state of total angular momentum J, z-projection M. If instead of 23 as the dipion we take 13 as the dipion, we will have a different set of angles $\Omega_2 = (\theta_2, \varphi_2)$,

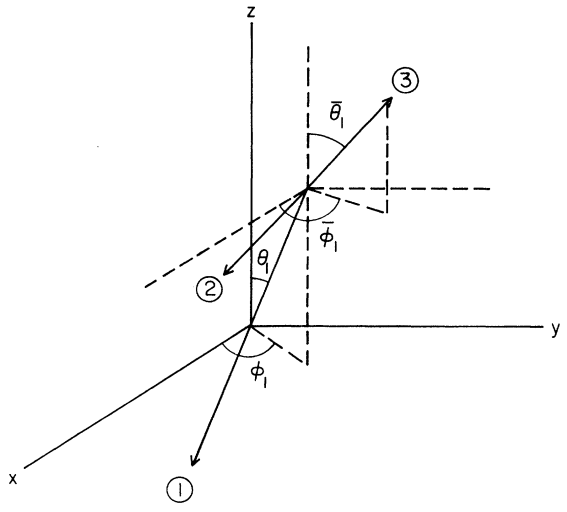

FIG. 3. Angles representing decay of 3π system into a dipion and a single π: (θ_1, φ_1); and those representing the subsequent decay of the dipion in its rest frame: $(\overline{\theta}_1, \overline{\varphi}_1)$.

$\overline{\Omega}_2 = (\overline{\theta}_2, \overline{\varphi}_2)$, and a different complete set of angular momentum states $Z_{LS}^{JM}(\Omega_2, \overline{\Omega}_2)$. Under interchange of the two identical π^-'s 1 and 2, $Z_{LS}^{JM}(\Omega_1, \overline{\Omega}_1) \rightleftarrows Z_{LS}^{JM}(\Omega_2, \overline{\Omega}_2)$. Using these angular momentum states we can express the amplitudes T_{JMP} in the form

$$T_{JMP} = \sum_{LS} F_{LS}^{JM}(s_1) Z_{LS}^{JM}(\Omega_1, \overline{\Omega}_1) . \tag{2.2}$$

This is meant to apply to the process of Fig. 1(a); S is the spin of the dipion $\pi_2^- \pi_3^+$. The Bose symmetrization to include the term corresponding to Fig. 1(b) will be done later when probability distributions are calculated.

It is also convenient to introduce helicity amplitudes f_λ^{JMP}. In terms of these the matrix element T_{JMP} given by (2.2) can be expressed as

$$T_{JMP} = \sum_{\lambda} f_\lambda^{JMP}(s_1, s_2) \left(\frac{2J+1}{8\pi^2} \right)^{1/2} D_{M\lambda}^{J*}(\alpha, \beta, \gamma) . \tag{2.3}$$

Here s_1, s_2 are Dalitz plot variables, $D_{M\lambda}^J$ is a Wigner rotation function, and α, β, γ are the Euler angles describing the rotation which carries the three pion system with fixed s_1, s_2 from a standard reference configuration to the actual configuration. The reference configuration is arbitrary; we take it to be that configuration in which particle π_1^- is moving in the $-z$ direction and particle π_3^+ is moving in the xz plane with a positive x component of its momentum. The z axis is always chosen to be in the direction of motion of the incoming pion in the three-pion center-of-mass frame. In this frame the reaction takes place in the xz plane and the initial and final nucleons have negative x components of momentum. The conventions defining the x and z axes are recorded in Figs. 4(a) and 4(b). The standard reference configuration for the three pions is given in Fig. 4(c).

We also need the relation between the LS amplitudes and the helicity amplitudes. To establish this, equate the right-hand sides of (2.2) and (2.3) and notice that applying the raising or lowering operators $(J_x \pm iJ_y)^n$ leads to a more general relation:

$$\sum_{\lambda} f_\lambda^{JMP}(s_1, s_2) \left(\frac{2J+1}{8\pi^2} \right)^{1/2} D_{M'\lambda}^{J*}(\alpha, \beta, \gamma) = \sum_{LS} F_{LS}^{JM} Z_{LS}^{JM'}(\Omega_1, \overline{\Omega}_1) , \tag{2.4}$$

in which M and M' are independent. We now evaluate (2.4) in the limit when the rotation $(\alpha, \beta, \gamma) = (0, 0, 0)$ is no rotation at all. In this limit $D_{M'\lambda}^J(\alpha, \beta, \gamma) = \delta_{M'\lambda}$. Comparing Figs. 3 and 4(c) we see that $\theta_1 = 0$, $\overline{\varphi}_1 = 0$, $\theta_1 = \chi_1$. The angle χ_1 is indicated in Fig. 4(c); it is measured in the dipion $\pi_2^- \pi_3^+$ center-of-mass frame. Using $Y_L^{M_L}(\theta_1, \varphi_1)$

$= [(2L+1)/4\pi]^{1/2}\delta_{M_L 0}$, $Y_S^M s(\bar{\theta}_1, \bar{\varphi}_1) = [(2S+1)/4\pi]^{1/2} \times d^S_{M_S 0}(\chi_1)$, and (2.1) we find that (2.4) reduces to

$$f_\lambda^{JMP}(s_1, s_2) = \sum_{LS} F_{LS}^{JM}(s_1)\left(\frac{2L+1}{2J+1}\right)^{1/2}\langle J\lambda | LS0\lambda\rangle \times\left(\frac{2S+1}{2}\right)^{1/2} d^S_{\lambda 0}(\chi_1). \quad (2.5)$$

In order finally to obtain the angular momentum decomposition in the form desired, we substitute (2.5) in (2.3), identify β and α with the polar and azimuthal angles θ_1, φ_1 of the dipion, and combine the factor $e^{i\lambda\gamma}$ from $D^{J*}_{M\lambda}(\alpha, \beta, \gamma)$ with the function $d^S_{\lambda 0}(\chi_1)$. If we also sum over all states JMP, and include indices $\rho\sigma$ to describe the helicity states of the nucleons, we obtain the general angular momentum decompositon of the matrix element for the process $\pi^- p \to \pi^+\pi^-\pi^- p$:

$$T_{\rho\sigma} = \sum_{JMLS} F^{JM}_{LS,\rho\sigma}\sum_\lambda \left(\frac{2L+1}{2J+1}\right)^{1/2}\langle J\lambda | LS0\lambda\rangle \times\left(\frac{2J+1}{2\pi}\right)^{1/2} D^{J*}_{M\lambda}(\varphi_1, \theta_1, 0) \times\left(\frac{2S+1}{4\pi}\right)^{1/2} D^{S*}_{\lambda 0}(\gamma, \chi_1, 0). \quad (2.6)$$

Note that $F^{JM}_{LS,\rho\sigma}(s, t, W, s_1)$ is a function of the angular momentum indices indicated and also the invariants $s = (p_A + p_B)^2$, $t = (p_B - p_D)^2$, $W^2 = (p_1 + p_2 + p_3)^2$, and $s_1 = (p_2 + p_3)^2$ [the names of the particles are indicated in Fig. 4(a)].

It is clear that it would be quite complicated to extract the partial-wave amplitudes $F^{JM}_{LS,\rho\sigma}$ from an arbitrary formula for T. For the generalized Deck model there are some substantial simplifications compared to the general case. The invariant matrix element for production of a dipion state $\pi_2^-\pi_3^+$ with spin S is

$$T_{S,\rho\sigma} = \frac{8\pi\sqrt{s_1}}{q_1}\frac{1}{2i}[\eta_S(s_1)e^{2i\delta_S(s_1)} - 1](2S+1)P_S(\theta_{\pi\pi}) \times(\text{pion propagator}) \times(\pi N \text{ scattering amplitude})_{\rho\sigma}. \quad (2.7)$$

Here $\theta_{\pi\pi}$ is the scattering angle between the incident pion A and the outgoing pion π_2^- in the $\pi_2^-\pi_3^+$ rest frame. To extract the partial-wave amplitudes, we must reexpress $P_S(\theta_{\pi\pi})$ in terms of the angles γ, χ_1 used in Eq. (2.6).

If we define a new angle ψ, the angle between the direction of the dipion in the 3π rest frame and the direction of the z axis (direction of incoming pion momentum) in the dipion rest frame, then clearly composition of rotations gives

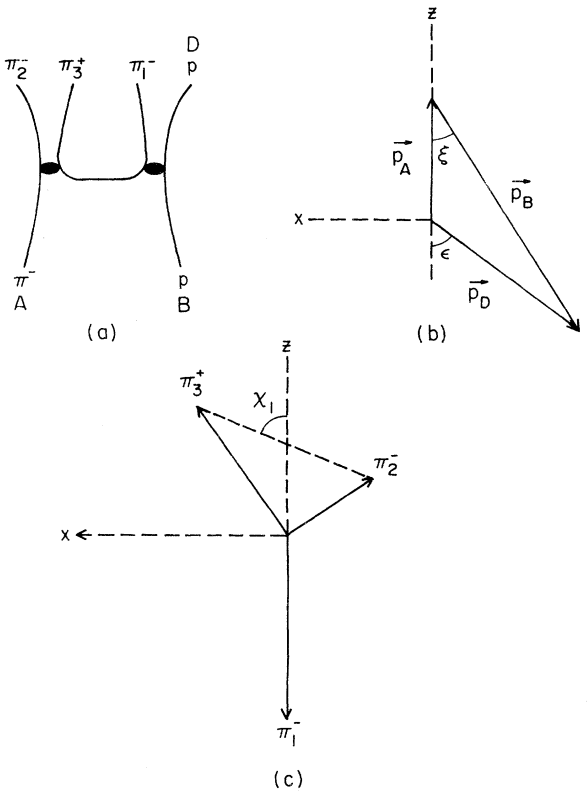

FIG. 4. (a) and (b): definition of momentum vectors and the xz plane in 3π rest frame; (c) standard reference frame for the three pions.

$$P_S(\theta_{\pi\pi}) = D^{S*}_{00}(0, \theta_{\pi\pi}, 0) = (-1)^S\sum_\lambda d^S_{0\lambda}(\psi)D^{S*}_{\lambda 0}(\gamma, \chi_1, 0). \quad (2.8)$$

The factor $(-1)^S$ enters because $\theta_{\pi\pi}$ is the angle between the two π^- mesons, whereas with our conventions γ, χ_1 give the orientation of the π^+ me-

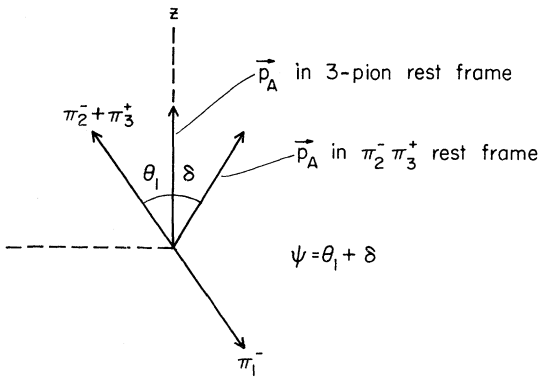

FIG. 5. Definition of angles between incident π^- and outgoing dipion in two frames.

son. We may reexpress ψ in terms of angles already defined by examining the Lorentz transformation from the three-pion rest frame to the dipion $\pi_2^-\pi_3^+$ rest frame, represented in Fig. 5. The angle θ_1, which gives the orientation of the dipion momentum relative to the incoming pion direction in the three-pion rest frame, transforms to $\psi = \theta_1 + \delta$.

Substituting (2.8) in (2.7) and comparing with (2.6) we then find

$$\sum_{JLM} F^{JM}_{LS,\rho\sigma}\left(\frac{2L+1}{2J+1}\right)^{1/2}\langle J\lambda|LS0\lambda\rangle\left(\frac{2J+1}{4\pi}\right)^{1/2} D^{J*}_{M\lambda}(\varphi_1,\theta_1,0)\left(\frac{2S+1}{4\pi}\right)^{1/2}$$
$$= \frac{8\pi\sqrt{s_1}}{q_1}\frac{1}{2i}[\eta_S(s_1)e^{2i\delta_S(s_1)}-1](2S+1)(-1)^S d^S_{0\lambda}(\psi)$$
$$\times(\text{pion propagator})(\pi N \text{ scattering amplitude})_{\rho\sigma}. \quad (2.9)$$

Multiplying both sides of (2.9) by $D^J_{M\lambda}(\varphi_1,\theta_1,0)$ and integrating yields

$$\sum_L F^{JM}_{LS,\rho\sigma}\frac{[(2L+1)(2S+1)]^{1/2}}{2J+1}\langle J\lambda|LS0\lambda\rangle = \frac{8\pi\sqrt{s_1}}{q_1}\frac{1}{2i}[\eta_S(s_1)e^{2i\delta_S(s_1)}-1]$$
$$\times(2S+1)(-1)^S\int_0^{2\pi}d\varphi_1\int_{-1}^{+1}d\cos\theta_1 D^J_{M\lambda}(\varphi_1,\theta_1,0)d^S_{0\lambda}(\psi)$$
$$\times(\text{pion propagator})(\pi N \text{ scattering amplitude})_{\rho\sigma}. \quad (2.10)$$

We can now use the orthogonality property

$$\sum_\nu\left(\frac{2L+1}{2J+1}\right)^{1/2}\langle J\nu|LS0\nu\rangle\left(\frac{2L'+1}{2J+1}\right)^{1/2}\langle J\nu|L'S0\nu\rangle = \delta_{LL'} \quad (2.11)$$

to undo the sum over L in (2.10) and finally obtain

$$F^{JM}_{LS,\rho\sigma} = \frac{8\pi\sqrt{s_1}}{q_1}[(2L+1)(2S+1)]^{1/2}\frac{1}{2i}[\eta_S(s_1)e^{2i\delta_S(s_1)}-1](-1)^S\sum_\lambda\langle J\lambda|LS0\lambda\rangle\int_{-1}^{+1}d\cos\theta_1 d^J_{M\lambda}(\theta_1)d^S_{0\lambda}(\psi)$$
$$\times(\text{pion propagator})\int_0^{2\pi}d\varphi_1 e^{-iM\varphi_1}(\pi N \text{ scattering amplitude})_{\rho\sigma}. \quad (2.12)$$

This formula can be written in a different but equivalent form by using $\psi = \delta + \theta_1$ (see Fig. 5), $d^S_{0\lambda}(\psi) = \sum_\mu d^S_{0\mu}(\delta)d^S_{\mu\lambda}(\theta_1)$, and the Clebsch-Gordan series for the product $d^J_{M\lambda}(\theta_1)d^S_{\mu\lambda}(\theta_1)$. One finds that

$$F^{JM}_{LS,\rho\sigma} = \frac{8\pi\sqrt{s_1}}{q_1}[(2L+1)(2S+1)]^{1/2}\frac{1}{2i}[\eta_S(s_1)e^{2i\delta_S(s_1)}-1](-1)^S\sum_\mu\langle JM|LS\,M-\mu\,\mu\rangle$$
$$\times\int_{-1}^{+1}d\cos\theta_1 d^S_{0\mu}(\delta)d^L_{M-\mu\,0}(\theta_1)(\text{pion propagator})\int_0^{2\pi}d\varphi_1 e^{-iM\varphi_1}(\pi N \text{ scattering amplitude})_{\rho\sigma}. \quad (2.13)$$

We see that the simple behavior of the Deck-model amplitude, in particular the way in which the $\pi\pi$ scattering factors off, has reduced the number of integrals which must be performed to two. Furthermore, the assumptions we have made about using on-shell $\pi\pi$ and πN scattering amplitudes with only helicity-zero couplings for the exchanged Reggeized pion have resulted in the dependence on φ_1 being entirely in the πN scattering amplitude. These simplifications make the numerical calculation of (2.12) or (2.13) quite feasible.

The first part of our calculation consists of numerical evaluation of the formula (2.12) and construction of a large table of answers.

B. Cross Sections

In order to calculate cross sections from the partial-wave amplitudes we must reassemble the partial-wave series and perform the Bose symmetrization ($\pi_1^- \leftrightarrow \pi_2^-$). It seems easiest to work with the helicity amplitudes given by (2.3), (2.5). We thus find for the complete Bose-symmetrized matrix element

$$T_{\rho\sigma} = \sum_{JMP\lambda}\left(\frac{2J+1}{8\pi^2}\right)^{1/2} D^{J*}_{M\lambda}(\alpha,\beta,\gamma)\left[f^{JMP}_{\lambda,\rho\sigma}(s_1,s_2)+\sum_\nu(-1)^\nu d^J_{\lambda\nu}(\theta_{12})f^{JMP}_{\nu,\rho\sigma}(s_2,s_1)\right], \quad (2.14)$$

where the helicity amplitudes are given in terms of the LS amplitudes by

$$f^{JMP}_{\lambda,\rho\sigma}(s_1,s_2)=\sum_{LS}F^{JM}_{LS,\rho\sigma}(s_1)\left(\frac{2L+1}{2J+1}\right)^{1/2}\langle J\lambda|LS0\lambda\rangle \times\left(\frac{2S+1}{2}\right)^{1/2}d^{S}_{\lambda 0}(\chi_1), \quad (2.15)$$

$$f^{JMP}_{\nu,\rho\sigma}(s_2,s_1)=\sum_{LS}F^{JM}_{LS,\rho\sigma}(s_2)\left(\frac{2L+1}{2J+1}\right)^{1/2}\langle J\nu|LS0\nu\rangle \times\left(\frac{2S+1}{2}\right)^{1/2}d^{S}_{\nu 0}(\chi_2). \quad (2.16)$$

(Here we suppress the other arguments of $F^{JM}_{LS,\rho\sigma}$ for convenience.)

The geometrical quantities are indicated in the "velocity diagram" of Fig. 6. The angle θ_{12} is measured in the three-pion center-of-mass frame, χ_1 is measured in the dipion $\pi_2^-\pi_3^+$ center-of-mass frame, and χ_2 is measured in the dipion $\pi_1^-\pi_3^+$ center-of-mass frame. It is easy to understand the factors $(-1)^\nu d^J_{\lambda\nu}(\theta_{12})$ in (2.14) which arise when one interchanges the two particles π_1^- and π_2^-. Suppose for example that $\alpha=\beta=\gamma=0$. Then the particles described by the first term in the square bracket of (2.14) are in the standard reference configuration, as described after Eq. (2.3), with particle π_1^- moving in the $-z$ direction. After the interchange, particle π_2^- is moving in the $-z$ direction. This latter configuration is obtained from the standard configuration by a rotation through 180° about the z axis followed by a rotation through a positive angle θ_{12} about the y axis.

We can now proceed to the calculation of the cross section for $\pi^-p\to\pi^-\pi^+\pi^-p$ using the relation between the invariant matrix element T and the

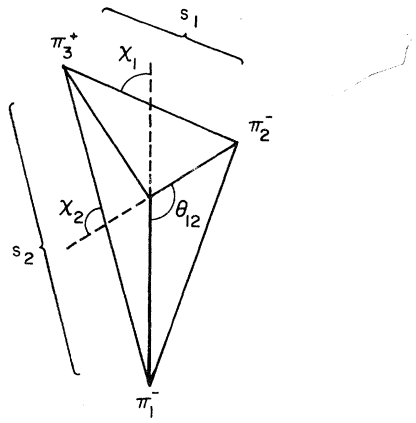

FIG. 6. Mnemonic for the angles χ_1, χ_2, θ_{12}. χ_1 is the angle between $\vec{p}_2-\vec{p}_3$ and $\vec{p}_1$ in the rest frame of $\vec{p}_2+\vec{p}_3$; χ_2 is the angle between $\vec{p}_3-\vec{p}_1$ and $\vec{p}_2$ in the rest frame of $\vec{p}_1+\vec{p}_3$; θ_{12} is the angle between $\vec{p}_1$ and $\vec{p}_2$ in the three-pion rest frame.

S matrix:

$$S=i(2\pi)^4\delta^4(p_A+p_B-p_D-p_1-p_2-p_3)\times\frac{T}{(2^6E_AE_BE_DE_1E_2E_3)^{1/2}}, \quad (2.17)$$

and the expression for four-body phase space:

$$\delta^4(p_A+p_B-p_D-p_1-p_2-p_3)\frac{d^3p_D}{E_D}\frac{d^3p_1}{E_1}\frac{d^3p_2}{E_2}\frac{d^3p_3}{E_3} =\frac{2\pi}{8p_{\rm lab}m_p}d\alpha\,d\cos\beta\,d\gamma\,ds_1ds_2dt\,\frac{dW}{W}. \quad (2.18)$$

Using the orthogonality properties of the $D^J_{M\lambda}(\alpha,\beta,\gamma)$ it is trivial to integrate over the external angles α,β,γ. We find that

$$\frac{d\sigma}{dW\,dt}=\frac{\pi}{(4\pi)^8}\left(\frac{\hbar c}{p_{\rm lab}m_p}\right)^2\frac{1}{W}\frac{1}{2!}\sum_{JMP\lambda}\frac{1}{2}\sum_{\rho\sigma}\int ds_1\int ds_2\left|f^{JMP}_{\lambda,\rho\sigma}(s_1,s_2)+\sum_\nu(-1)^\nu d^J_{\lambda\nu}(\theta_{12})f^{JMP}_{\nu,\rho\sigma}(s_2,s_1)\right|^2. \quad (2.19)$$

Here the 2! is the usual factor which arises when we have two identical particles. In (2.19) the noninterference of states with different $JM\lambda$ follows from the orthogonality of the Wigner $D^J_{M\lambda}$ functions. The noninterference of states with different parity follows, after summation over $\pm\lambda$, from the parity identity

$$f^{JMP}_{-\lambda,\rho\sigma}(s_1,s_2)=P(-1)^{J-\lambda-1}f^{JMP}_{\lambda,\rho\sigma}(s_1,s_2), \quad (2.20)$$

which can be derived, for example, from (2.15).

To proceed further with the integration over the Dalitz plot in (2.19) we substitute the series (2.15) and (2.16) expressing the helicity amplitudes in terms of LS amplitudes. The integration over s_2 can then be transformed to an angular integration over χ_1, using the kinematic relation

$$s_2=\tfrac{1}{2}(W^2+3m_\pi^2-s_1)+2p_1q_1\frac{W}{\sqrt{s_1}}\cos\chi_1, \quad (2.21)$$

where p_1 is the relative momentum in the pion 1 + dipion 23 system:

$$p_1=\frac{1}{2W}\{[(W-m_\pi)^2-s_1][(W+m_\pi)^2-s_1]\}^{1/2}, \quad (2.22)$$

and q_1 is the relative momentum in the dipion 23 system:

$$q_1 = \tfrac{1}{2}(s_1 - 4m_\pi{}^2)^{1/2}. \tag{2.23}$$

There are two kinds of terms in (2.19), the direct and the cross terms. Using the orthogonality properties of the $d^S_{\lambda 0}(\cos\chi_1)$ and the orthogonality relation (2.11) the direct terms are easily reduced to single integrals:

$$\sum_\lambda \int ds_1 \int ds_2 |f^{JMP}_{\lambda,\rho\sigma}(s_1, s_2)|^2 = \sum_\lambda \int ds_1 \int ds_2 \left| \sum_\nu (-1)^\nu d^J_{\lambda\nu}(\theta_{12}) f^{JMP}_{\nu,\rho\sigma}(s_2, s_1) \right|^2$$
$$= \sum_{LS} \int_{(2m_\pi)^2}^{(W-m_\pi)^2} ds_1 \frac{2p_1 q_1 W}{\sqrt{s_1}} |F^{JM}_{LS,\rho\sigma}(s_1)|^2. \tag{2.24}$$

In a similar way the cross term can be reduced to

$$2\mathrm{Re} \sum_\lambda \int ds_1 \int ds_2 f^{JMP}_{\lambda,\rho\sigma}(s_1, s_2) \sum_\nu (-1)^\nu d^J_{\lambda\nu}(\theta_{12}) f^{JMP*}_{\nu}(s_2, s_1)$$
$$= \sum_{L_a S_a} \sum_{L_b S_b} \int_{(2m_\pi)^2}^{(W-m_\pi)^2} ds_1 \frac{2p_1 q_1 W}{\sqrt{s_1}} \int_{-1}^{+1} d\cos\chi_1 K_{ab}(1, 2) 2\mathrm{Re} F^{JM}_{L_a S_a,\rho\sigma}(s_1) F^{JM*}_{L_b S_b,\rho\sigma}(s_2), \tag{2.25}$$

where

$$K_{ab}(1, 2) = \sum_{\nu_a \nu_b} C(J, L_a, S_a, \nu_a) C(J, L_b, S_b, \nu_b)$$
$$\times (-1)^{\nu_b} d^{S_a}_{\nu_a 0}(\chi_1) d^J_{\nu_a \nu_b}(\theta_{12}) d^{S_b}_{\nu_b 0}(\chi_2) \tag{2.26}$$

and

$$C(J, L, S, \nu) = \left(\frac{(2L+1)(2S+1)}{2(2J+1)} \right)^{1/2} \langle J\nu | LS0\nu \rangle. \tag{2.27}$$

We note the presence of nonvanishing interference terms between states with different LS but the same JMP in the cross terms (2.25).

The results for individual angular momentum states given in Sec. III were calculated numerically using the above formulas. It is not feasible to calculate in this way the total cross section as the sum over all angular momentum components. This is so because the Deck model yields a small but non-negligible tail of states with large L. Consequently such total cross sections were calculated with a Monte Carlo method — the same method as used in paper II, except here with the two-diagram model.

C. Nuclear Helicity Amplitudes

There are a number of interesting matters to discuss under this heading. Most of these have been left to Sec. V of the paper. Here we merely list the somewhat inelegant formulas actually used in the numerical computation. As discussed in the Introduction, the πN $\mathcal{A}$ and $\mathcal{B}$ amplitudes are calculated from either the phase shifts or the Barger-Phillips formulas, depending on the energy. In terms of these the invariant πN scattering amplitude is given by

$$\mathfrak{N} = \bar{u}(p_D)[\mathcal{A} - i\gamma \cdot \tfrac{1}{2}(Q + p_1)\mathcal{B}]u(p_B)$$
$$= \bar{u}(p_D)[\mathcal{A} - i\gamma \cdot p_1 \mathcal{B}]u(p_B) \tag{2.28}$$

when the 4-momentum Q of the virtual exchanged pion is eliminated in favor of the 4-momentum p_1 of the final pion, using momentum conservation and the properties of the Dirac equation. The helicity amplitudes are evaluated from (2.28).

We work in the same center-of-mass system for the final three pions as used in the discussion leading to (2.12). The following combinations of helicity amplitudes are even or odd in φ_1:

$$\tfrac{1}{2}(\mathfrak{N}_{++} + \mathfrak{N}_{--}) = (Y\mathcal{A} + XE_1\mathcal{B})\cos\tfrac{1}{2}(\epsilon - \xi)$$
$$- Up_1\mathcal{B}[\cos\tfrac{1}{2}(\epsilon + \xi)\cos\theta_1$$
$$+ \sin\tfrac{1}{2}(\epsilon + \xi)\sin\theta_1\cos\varphi_1],$$

$$\tfrac{1}{2}(\mathfrak{N}_{+-} - \mathfrak{N}_{-+}) = -(X\mathcal{A} + YE_1\mathcal{B})\sin\tfrac{1}{2}(\epsilon - \xi)$$
$$- Vp_1\mathcal{B}[\sin\tfrac{1}{2}(\epsilon + \xi)\cos\theta_1$$
$$-\cos\tfrac{1}{2}(\epsilon + \xi)\sin\theta_1\cos\varphi_1], \tag{2.29}$$

$$\frac{1}{2i}(\mathfrak{N}_{++} - \mathfrak{N}_{--}) = Up_1\mathcal{B}\sin\tfrac{1}{2}(\epsilon - \xi)\sin\theta_1\sin\varphi_1,$$

$$\frac{1}{2i}(\mathfrak{N}_{+-} + \mathfrak{N}_{-+}) = Vp_1\mathcal{B}\cos\tfrac{1}{2}(\epsilon - \xi)\sin\theta_1\sin\varphi_1,$$

where

$$X = [(E_B + m_p)(E_D + m_p)]^{1/2} + [(E_B - m_p)(E_D - m_p)]^{1/2},$$
$$Y = [(E_B + m_p)(E_D + m_p)]^{1/2} - [(E_B - m_p)(E_D - m_p)]^{1/2},$$
$$U = [(E_B + m_p)(E_D - m_p)]^{1/2} + [(E_B - m_p)(E_D + m_p)]^{1/2},$$
$$V = [(E_B + m_p)(E_D - m_p)]^{1/2} - [(E_B - m_p)(E_D + m_p)]^{1/2}.$$

The angles ϵ and ξ give the orientation of $\vec{p}_D$ and $\vec{p}_B$ with respect to the negative z axis as shown in

Fig. 4(b).

The kinematic formulas are a little strange in the three-pion rest frame. We list here those formulas needed for the computation. In terms of the invariants $s=(p_A+p_B)^2$, $t=(p_B-p_D)^2$, $W^2=(p_1+p_2+p_3)^2$, and $s_1=(p_2+p_3)^2$ we find that

$$
\begin{aligned}
E_A &= \frac{W^2+m_\pi{}^2-t}{2W}, \\
E_D &= \frac{s-W^2-m_p{}^2}{2W}, \\
E_B &= E_D+W-E_A, \\
\cos\epsilon &= \frac{p_B{}^2-p_D{}^2-p_A{}^2}{2p_D p_A}, \\
\cos\xi &= \frac{p_D\cos\epsilon+p_A}{p_B}, \\
E_1 &= \frac{W^2+m_\pi{}^2-s_1}{2W}, \\
s_{\pi N} &= m_\pi{}^2+m_p{}^2+2E_D E_1 \\
&\quad -2p_D p_1(\cos\epsilon\cos\theta_1+\sin\epsilon\sin\theta_1\cos\varphi_1), \\
t_R &= m_\pi{}^2+s_1-2E_A(W-E_1)+2p_A p_1\cos\theta_1, \\
\tan\psi &= \frac{\sqrt{s_1}\,p_A\sin\theta_1}{(W-E_1)p_A\cos\theta_1-p_1E_A}.
\end{aligned}
\tag{2.30}
$$

The center-of-mass frame scattering angle for the πN scattering is

$$
\cos\theta_{\text{c.m.}}=\frac{t-t_R-m_\pi{}^2+2E_RE_V}{2Q_RQ_V},
$$

where Q_R, E_R and Q_V, E_V are the center-of-mass momentum and energy for, respectively, the final real πN and the initial virtual πN:

$$
E_R=\frac{s_{\pi N}+m_\pi{}^2-m_p{}^2}{2(s_{\pi N})^{1/2}}, \quad Q_R=(E_R{}^2-m_\pi{}^2)^{1/2},
$$

$$
E_V=\frac{s_{\pi N}+t_R-m_p{}^2}{2(s_{\pi N})^{1/2}}, \quad Q_V=(E_V{}^2-t_R)^{1/2}.
$$

From all these formulas we see that, aside from the explicit $\sin\varphi_1$ and $\cos\varphi_1$ in (2.29), φ_1 enters only via $\cos\varphi_1$ in $s_{\pi N}$. Therefore, from (2.29) $\mathfrak{N}_{++}+\mathfrak{N}_{--}$ and $\mathfrak{N}_{+-}-\mathfrak{N}_{-+}$ are even in φ_1, while $\mathfrak{N}_{++}-\mathfrak{N}_{--}$ and $\mathfrak{N}_{+-}+\mathfrak{N}_{-+}$ are odd in φ_1. It then follows from (2.12) that the partial-wave amplitudes with $M=0$ corresponding to the helicity combinations $\mathfrak{N}_{++}-\mathfrak{N}_{--}$ and $\mathfrak{N}_{+-}+\mathfrak{N}_{-+}$ will vanish identically. For the other helicity combinations corresponding to $\mathfrak{N}_{++}+\mathfrak{N}_{--}$ and $\mathfrak{N}_{+-}-\mathfrak{N}_{-+}$ the $M=0$ partial-wave amplitudes vanish when $P=(-1)^J$. This follows from (2.12) and the identities $d^J_{0-\lambda}(\theta)=(-1)^\lambda d^J_{0\lambda}(\theta_1)$, $\langle J-\lambda|LS0-\lambda\rangle=(-1)^{J-L-S}\langle J\lambda|LS0\lambda\rangle$. We return to a more meaningful discussion of these symmetry relations in Sec. V.

We can also obtain from these explicit formulas some information on the relative size of the amplitudes corresponding to different nucleon helicity states at large s. For large s the pion nucleon scattering will be dominated by Pomeranchon exchange, and the asymptotic energy dependence of the $\mathfrak{A}$ and $\mathfrak{B}$ amplitudes at $t=0$ is $\mathfrak{A}\sim s_{\pi N}$, $\mathfrak{B}\sim$ const. Expanding (2.29), (2.30) for large s we then find at $t=0$ that

$$
\begin{aligned}
&\mathfrak{N}_{++}+\mathfrak{N}_{--}\sim s, \quad \mathfrak{N}_{++}-\mathfrak{N}_{--}\sim\text{const}, \\
&\mathfrak{N}_{+-}-\mathfrak{N}_{-+}\sim s, \quad \mathfrak{N}_{+-}+\mathfrak{N}_{-+}\sim 1/s.
\end{aligned}
\tag{2.31}
$$

Actually πN scattering satisfies approximate s-channel helicity conservation,[9] which implies $\mathfrak{A}\sim$ const instead of $s_{\pi N}$. This leads to the revised estimate for $t=0$:

$$
\begin{aligned}
&\mathfrak{N}_{++}+\mathfrak{N}_{--}\sim s, \quad \mathfrak{N}_{++}-\mathfrak{N}_{--}\sim\text{const}, \\
&\mathfrak{N}_{+-}-\mathfrak{N}_{-+}\sim\text{const}, \quad \mathfrak{N}_{+-}+\mathfrak{N}_{-+}\sim 1/s.
\end{aligned}
\tag{2.32}
$$

Substituting these results in (2.12) leads to the same estimates for the relative size of the corresponding partial-wave amplitudes.

III. NUMERICAL RESULTS

We first look at a simplified version of the Deck model which is easier to understand than the general case. If the πN scattering amplitude is approximated by a flat Pomeranchon with an exponential residue function, and we use a non-Regge-ized pion propagator, we find an amplitude

$$
\begin{aligned}
T &= (\text{pion propagator})(\pi N \text{ scattering amplitude}) \\
&\propto \frac{is_{\pi N}e^{at'}}{m_\pi{}^2-t_R}
\end{aligned}
\tag{3.1}
$$

to substitute in (2.12) or (2.13). Substituting from (2.30) for $s_{\pi N}$ and t_R one obtains a complicated formula which, because it has a pole just outside the physical region, looks as though it contains many angular momentum components. However, it was shown years ago by Stodolsky[12] that the complications in (3.1) cancel each other. Because of the rapid decrease with t of diffraction scattering it is reasonable to evaluate (3.1) in the forward direction. Stodolsky applied the well-known formula for $t_{\min}$ to the production of the three-pion system and also to the virtual pion-nucleon scattering to obtain

$$
\begin{aligned}
(\sqrt{-t})_{\min} &= \frac{m_p(W^2-m_\pi{}^2)}{s} \\
&= \frac{m_p(m_\pi{}^2-t_R)}{s_{\pi N}}.
\end{aligned}
\tag{3.2}
$$

Thus, in the forward direction (3.1) reduces to

$$
T=\frac{is}{W^2-m_\pi{}^2}.
\tag{3.3}
$$

The angular dependence has completely disappeared, as has the pole. We can substitute this simple result in (2.13). The φ_1 integration will force $M=0$. For small W, $\delta \to 0$ and $d^S_{0\mu}(\delta) \to \delta_{0\mu}$. The θ_1 integration then forces $L=0$. In this way we can understand that the dominant amplitude from a Deck-model calculation will have $L=0, M=0$. This is above and beyond the usual threshold factors p_1^L which tend to enhance low L relative to large L at low energies.

If we consider deviations from this simple version of the model, we see that there will be numerical problems which must be handled carefully. Deviations from a flat Pomeranchon with $\alpha=1$ imply an imperfect cancellation of the pole in the pion propagator. Referring to (2.12) and the formula for t_R [Eq. (2.30)] we see that the integrand for the θ_1 integration will be rapidly varying due to the pion pole. A similar problem arises from the dependence of πN scattering on $s_{\pi N}$. From the formula for $s_{\pi N}$ [Eq. (2.30)] we see that in the neighborhood of a certain (geographic) pole in the θ_1, φ_1 integration, near $\cos\epsilon \cos\theta_1 + \sin\epsilon \sin\theta_1 \cos\varphi_1 = 1$, $s_{\pi N}$ can be sufficiently small that we are in the resonance region for πN scattering, so that the πN scattering amplitudes are rapidly varying as functions of θ_1, φ_1. These rapid variations have two consequences: (a) A large number of integration points must be used to obtain an accurate answer; (b) there is a small but non-negligible tail of high-L states generated by the Deck model with realistic πN scattering, as used in this paper.

After all these explanations and cautions we now finally present some numerical results. In Fig. 7 we present cross sections integrated over all variables except the three-pion energy W. The curve labeled "Total" was calculated with a Monte Carlo method and represents a sum over all angular momentum components. The other curves in Fig. 7 were calculated with the formulas derived in Sec. II. The difference between the curve labeled "Sum" ($L \leq 3$, $S \leq 2$, $|M| \leq 1$) and the curve labeled "Total" is due to the tail of high angular momentum states alluded to above. Note that the difference grows with increasing W, as expected. The remaining curves in Fig. 7 give the contributions of those J^P states which make the largest contributions. Each J^P curve is itself a sum of contributions from several states with $L \leq 3$, $S \leq 2$, $|M| \leq 1$ and includes interference terms between states with different L, S but the same J^P, as explained in Sec. II B.

We note the dominant A_1 effect in the 1^+ state with a peak at about 1.125 GeV, consistent with experimental results for the A_1. There is also a small A_3 effect in the 2^- state, peaking at an energy of about 1.5 GeV, somewhat lower than the experimental result. The 2^- peak is too small to be noticeable in the curves Sum and Total.

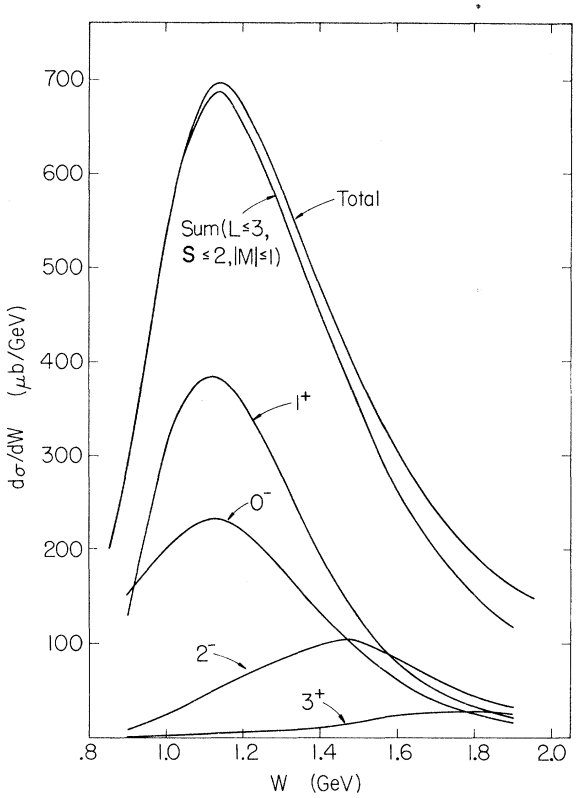

FIG. 7. Cross sections for the dominant J^P states, and the sum of cross section contributions for low L, S, and J are compared with the total cross section obtained by Monte Carlo summation. $P_{\text{lab}} = 16$ GeV/c. Only amplitudes with $M<2$ and only the nucleon helicity combination $F_{++} + F_{--}$ are used in calculating the contributions of definite J.

In Fig. 8 the leading J^P states are replotted and in addition we show the principal LS contributions to each J^P state. Other contributions and interference terms are small. The notation on these curves is somewhat symbolic and recalls to mind that $\pi\pi$ scattering is dominated by the ϵ, ρ, and f resonances. Thus $1^+s(\rho\pi)$ means $L=0$, $S=1$, etc. The solid curves in Fig. 8 were calculated from the formulas of Sec. II. The points with error bars are the result of applying the FIT program to Monte Carlo events generated according to the two-diagram Deck model. We return to comparison of these calculations in Sec. IV.

We see from Fig. 8 that the 0^- and 1^+ peaks are mainly $L=0$ effects, $0^-s(\epsilon\pi)$, and $1^+s(\rho\pi)$, respectively. The $1^+s(\rho\pi)$ peak is of course the famous A_1 effect. The small 2^- peak is partly $2^-s(f\pi)$ and partly $2^-p(\rho\pi)$.

So much for the W dependence of the cross sections integrated over t. We show one graph of the

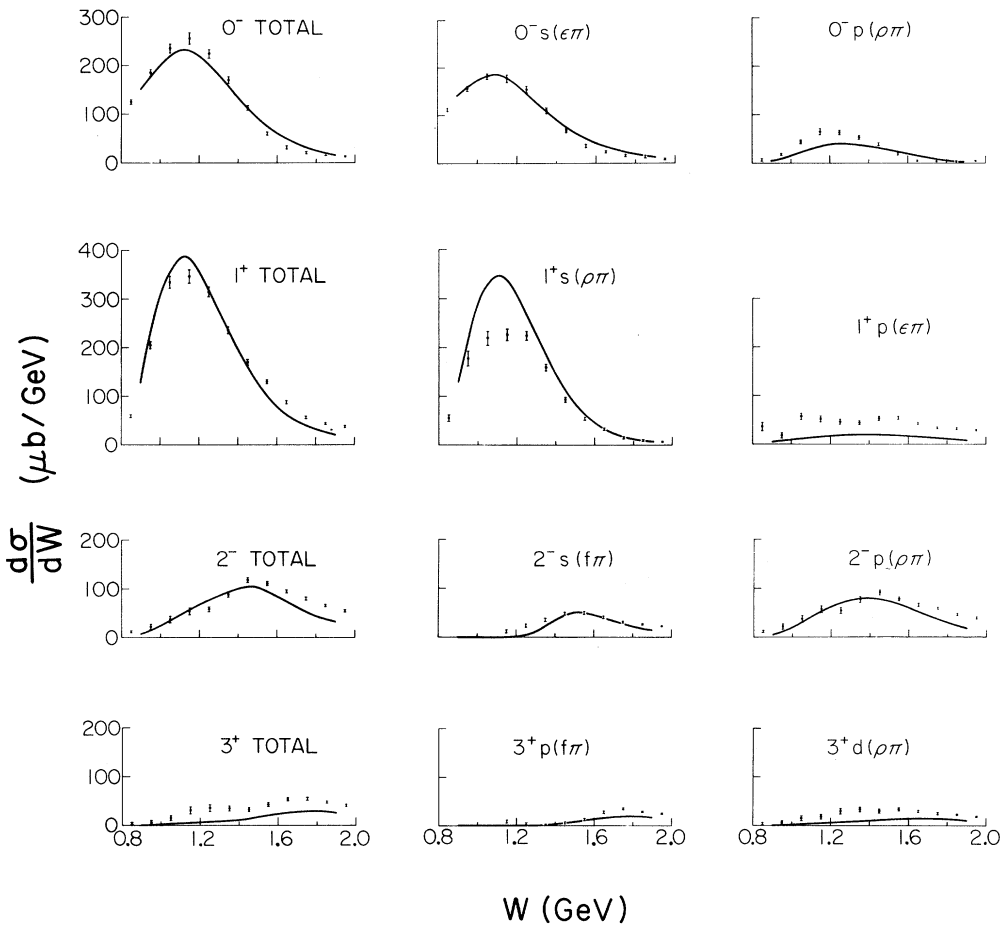

FIG. 8. Solid lines show cross-section contributions calculated with the formulas in the text. Points with error bars are the corresponding outputs obtained with the program FIT, using Monte Carlo events as input.

t dependence in Fig. 9. This plot was obtained from the Monte Carlo calculation and so contains a summation over all angular momentum components. Shown is $d\sigma/dt$ as a function of $t' = t - t_{\min}$ for three separate mass bins in W. The normalization was arbitrarily changed so that the curves start from the same value at $t' = 0$. We see that the slope decreases and the shape changes somewhat as W increases. Similar effects are observed in the individual angular momentum components as calculated by the methods of Sec. II. In general it is found that the slope decreases with increasing W for each angular momentum component, but not as much as indicated in Fig. 9 for the total. (We speak here of the dominant $M = 0$ partial-wave amplitudes. The smaller $M = 1$ amplitudes vanish at $t' = 0$.) At the same time the slope for the large magnitude low-L components is greater than for the large magnitude high-L components. The greater rate of decrease of the slope with W for the total is then due to the gradual shift from lower to higher L with increasing W.

The cross sections discussed above are integrals over the Dalitz plot of sums over helicity states of bilinear combinations of amplitudes, as discussed in Sec. II. To proceed further, in particular to discuss the question of phases, we must examine the individual amplitudes. These complex amplitudes $F^{JM}_{LS,\rho\sigma}$ as given by the formula (2.12) are functions of s, t, W, and s_1 as well as the angular momentum quantum numbers. As mentioned in Sec. II the calculation proceeds by making a large table of these amplitudes and then combining them to obtain cross sections. Part of one "page" from this large table is shown in Table I. (Actually in the table the multiplicative factor

$$\frac{8\pi\sqrt{s_1}}{q_1}\,\frac{1}{2i}[\eta_S(s_1)e^{2i\delta_S(s_1)} - 1](-1)^S \tag{3.4}$$

has been omitted.)

In Table I we have $s = 30.9$ GeV^2 corresponding to $p_{lab} = 16$ GeV, a typical $t' = -0.05$ GeV, $W = 1.1$ GeV near the A_1 peak, and $\sqrt{s_1} = 0.820$ GeV near the ρ mass. The dependence on the angular momentum quantum numbers and nucleon helicity indices is shown. As discussed at the end of Sec. II the $M = 0$ amplitudes for $J^P = 1^-, 2^+, \ldots$ are identically zero and these have been left out of the table. The $M = 0$ amplitudes for the nucleon helicity combinations $F_{++} - F_{--}$ and $F_{+-} + F_{-+}$ vanish identically for all J^P and are so given in the table.

We see confirmation of the predictions made for the relative sizes of the nucleon helicity combinations at large s [Eq. (2.32)]. The helicity combination $F_{++} + F_{--}$ is sufficiently dominant so that only it is kept in the cross-section calculations described above. As predicted at the beginning of this section, $L = 0$ and $M = 0$ (when allowed) dominate and amplitudes decrease with increasing L and M. Especially for the dominant amplitudes, the $M = 0$ component is usually much larger than the $M = 1$ component. Further checking has shown that amplitudes with $M \geq 2$ are negligible, and they have been omitted from the cross-section calculations.

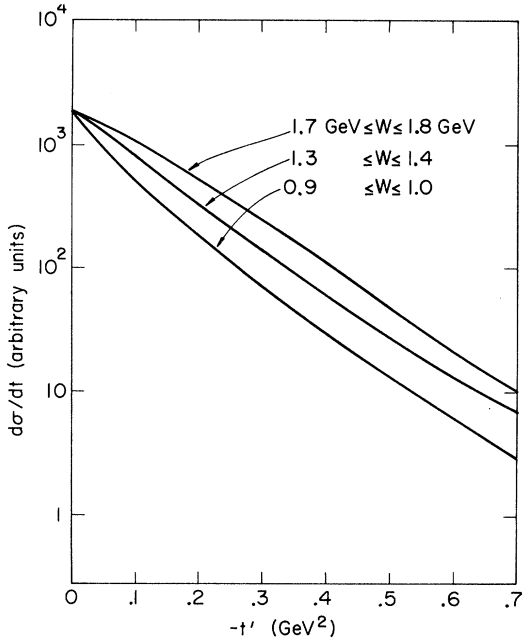

FIG. 9. Distribution of events in momentum transfer to the nucleon, as a function of 3π mass. All curves have been normalized to go through the same point at $t' = 0$.

TABLE I. Partial-wave amplitudes at $P_{lab} = 16$ GeV/c ($s = 30.9$ GeV^2), $t'_{NN} = -0.05$ (GeV/c)^2, $W = 1.1$ GeV, $s_1^{1/2} = 0.820$ GeV.

Quantum numbers of partial waves					$\frac{1}{2}(F_{++}+F_{--})$		$\frac{1}{2}(F_{+-}-F_{-+})$		$\frac{1}{2i}(F_{++}-F_{--})$		$\frac{1}{2i}(F_{+-}+F_{-+})$	
J	P	M	L	S	Magnitude[a]	Phase	Magnitude	Phase	Magnitude	Phase	Magnitude	Phase
0	−	0	0	0	20.12	129°	1.36	66°	0		0	
1	+	0	1	0	4.70	46°	0.32	74°	0		0	
1	+	1	1	0	2.46	129°	0.11	6°	0.09	−163°	0.01	17°
2	−	0	2	0	0.82	76°	0.45	101°	0		0	
2	−	1	2	0	0.99	123°	0.19	− 69°	0.05	−174°	0.01	6°
1	+	0	0	1	34.07	129°	2.30	67°	0		0	
1	+	1	0	1	0.65	− 51°	0.03	178°	0.02	16°	0.00	−164°
0	−	0	1	1	7.18	170°	0.09	5°	0		0	
1	−	1	1	1	3.10	129°	0.14	− 8°	0.11	−164°	0.02	16°
2	−	0	1	1	8.11	76°	0.70	69°	0		0	
2	−	1	1	1	2.76	129°	0.12	18°	0.10	−163°	0.02	18°
1	+	0	2	1	0.40	− 14°	0.48	− 76°	0		0	
1	+	1	2	1	0.35	− 63°	0.21	99°	0.03	− 2°	0.00	178°
2	+	1	2	1	0.94	126°	0.16	− 71°	0.04	−172°	0.01	8°
2	−	0	3	1	0.59	−130°	0.47	− 89°	0		0	
2	−	1	3	1	0.45	− 14°	0.34	81°	0.03	17°	0.00	−163°
2	−	0	0	2	42.01	129°	2.85	67°	0		0	
2	−	1	0	2	1.42	− 51°	0.06	177°	0.05	16°	0.01	−164°
1	+	0	1	2	13.39	158°	0.33	43°	0		0	
1	+	1	1	2	1.75	129°	0.09	− 33°	0.07	−165°	0.01	15°
2	+	1	1	2	3.89	129°	0.18	− 9°	0.14	−164°	0.02	16°
0	−	0	2	2	1.83	165°	0.48	100°	0		0	
1	−	1	2	2	0.25	− 63°	0.32	93°	0.03	− 5°	0.00	175°
2	−	0	2	2	0.66	106°	0.47	− 72°	0		0	
2	−	1	2	2	0.27	143°	0.10	92°	0.01	−101°	0	79°

[a] Magnitudes are expressed in arbitrary units. Also, the $\pi\pi$ scattering-amplitude factor has been removed from each partial wave.

In Figs. 10, 11, 12, and 13 we attempt to present some of the information contained in our large table on the variation with W and s_1 of certain partial-wave amplitudes at fixed s and t'. These are Argand plots of the real vs the imaginary parts of the dominant nuclear helicity amplitude $F_{++}+F_{--}$. The solid curves show the variation of the complex amplitude with W at fixed s_1. The dashed curves in Figs. 10 and 11 show the variation of the amplitude with s_1 at fixed W. In Figs. 10 and 11 the values chosen for s_1 correspond to the ρ mass and 50 MeV on either side of it and the f mass and 50 MeV on either side of it. In examining these curves, we must keep in mind that the variation

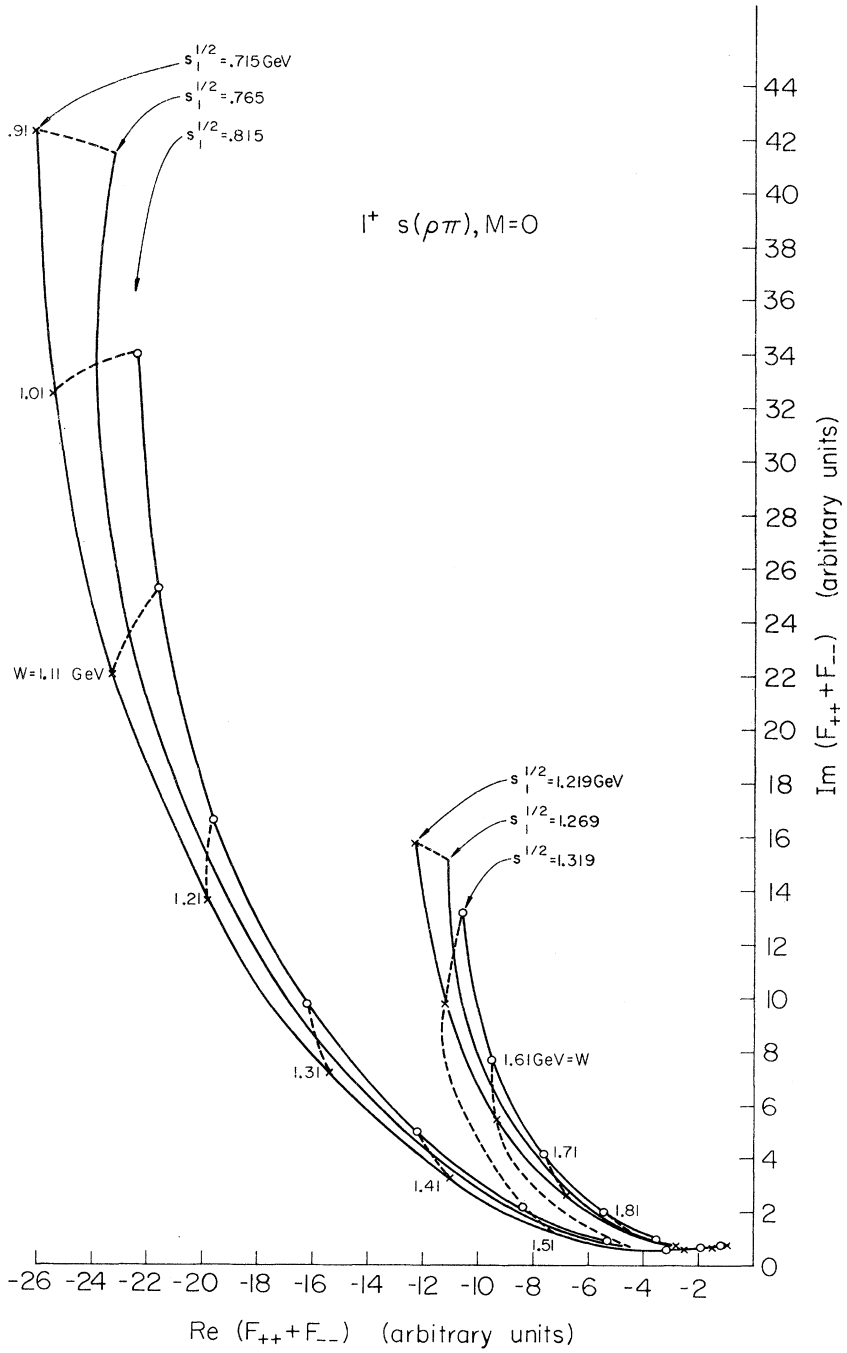

FIG. 10. Argand diagram for the 1^+s partial wave, as a function of s_1. P_{lab}= 16 GeV, t' = −0.05 GeV, M = 0.

due to the dipion resonances, contained in the factors (3.4), has been omitted.

In certain cases, Figs. 11 and 12, the Argand plot vs W is reminiscent of the corresponding plot for a two-body resonance. This type of variation seems to occur only for $L>0$; a barrier penetration factor ($\sim p^L$) which vanishes for $p \to 0$ seems necessary in order to pull the curve around into a circle. For a case with $L=0$, such as Fig. 10, the curve in flattened out and the phase variation is much less. In Fig. 13 we have the opposite extreme — the circle is distorted into a spike. The origin of these (sometime) circles in the Argand plot is the same as the origin of the famous Schmid circles[13] for Reggeized two-body amplitudes, namely, the variation of the Regge phase factor $\exp[-i\frac{1}{2}\pi\alpha(t_R)]$ incorporated in the Reggeized Deck model studied here [see Eq. (1.2)]. For the A_1 state $1^+s(\rho\pi)$ shown in Fig. 10 there is not very much phase variation, i.e., the A_1 does not behave like an ordinary resonant state, in agreement with the conclusions reached in fitting

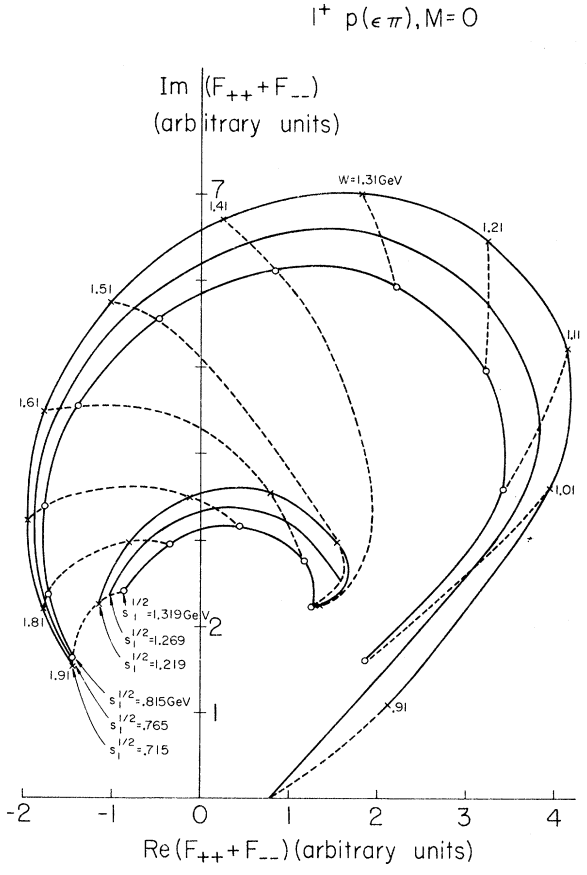

FIG. 11. Argand diagram for the 1^+p partial wave, as a function of s_1. $P_{\text{lab}}=16$ GeV, $t'=-0.05$ GeV, $M=0$.

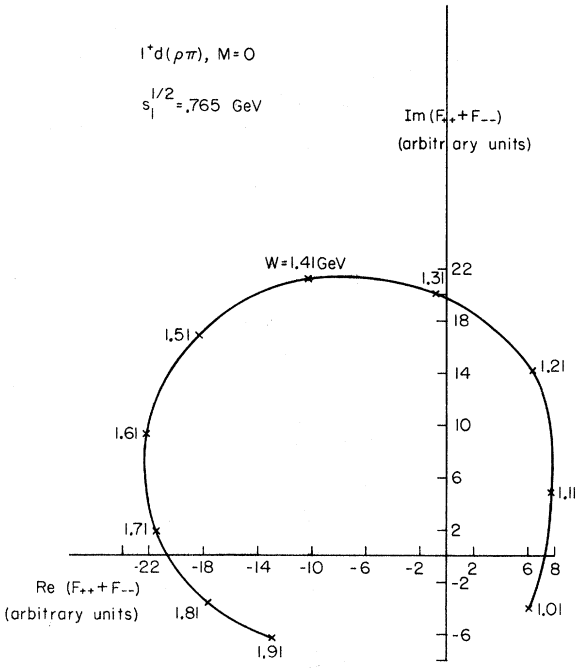

FIG. 12. Argand diagram for the 1^+d partial wave, at $s_1^{1/2}=0.765$ GeV. $P_{\text{lab}}=16$ GeV, $t'=-0.05$ GeV, $M=0$.

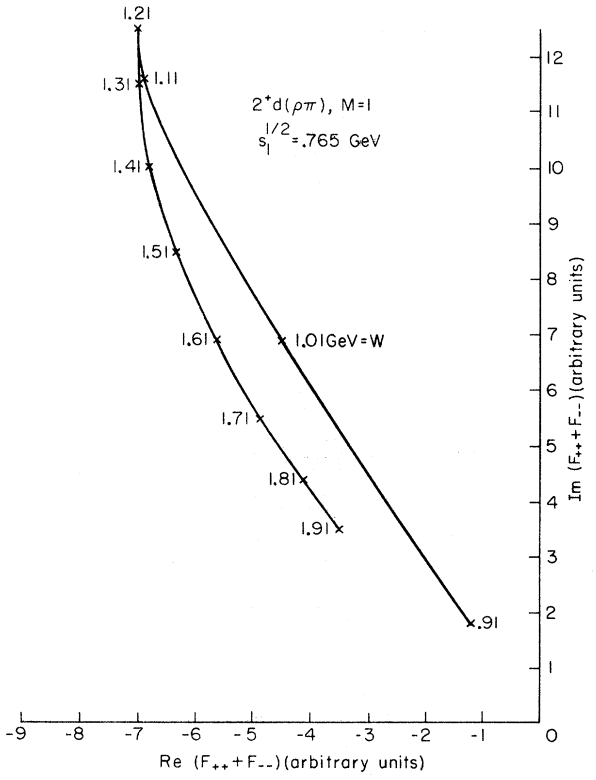

FIG. 13. Argand diagram for the 2^+d partial wave, at $s_1^{1/2}=0.765$ GeV. $P_{\text{lab}}=16$ GeV, $t'=-0.05$ GeV, $M=1$.

the experimental data. The $1^+p(\epsilon\pi)$ and $1^+d(\rho\pi)$ states plotted in Figs. 11 and 12 have the type of behavior usually associated with a very broad resonance but the magnitudes of these amplitudes are very tiny compared to the big amplitudes such as $1^+s(\rho\pi)$. (See Fig. 8.)

This phase information is presented differently in Figs. 14 and 15. In Fig. 14 we show the absolute phases of various partial-wave amplitudes (*sans* the $\pi\pi$ scattering amplitude) as a function of W for $p_{\text{lab}} = 16$ GeV, $t' = -0.05$ GeV, and $s_1^{1/2} = 1.269$ GeV = the f mass for the state $2^-s(f\pi)$, and $s_1^{1/2} = 0.765$ GeV = the ρ mass for the other cases. There would seem to be no evidence for resonant phase variation in Fig. 14.

In Fig. 15 the solid curves are differences between the absolute phases of Fig. 14. The points with error bars are the result of applying the program FIT to Monte Carlo events generated according to the two-diagram Deck model. The solid curves were calculated for a definite $t' = -0.05$ GeV and a definite $s_1^{1/2} = 0.765$ GeV or 1.269 GeV. The results from FIT represent, of course, a complicated average over t' and s_1. We return to a comparison of the two types of calculation in Sec. IV.

IV. COMPARISON WITH FIT

In the program FIT the reaction (1.1) is treated as a two-stage process, the production of a state with quantum numbers JMP followed by decay of this state. Thus the distribution in angles and energies of the three pions on the right-hand side of (1.1) is given by a formula of the type

$$\sum_{JMP}\sum_{J'M'P'} \mathfrak{M}_{J'M'P'}\rho_{J'M'P',\,JMP}\mathfrak{M}^*_{JMP}, \tag{4.1}$$

where $\rho_{J'M'P',\,JMP}$ is a density matrix describing the *production* of the three-pion state with quantum numbers JMP.

FIT makes some plausible but not completely general assumptions about the matrix element $\mathfrak{M}_{JMP}$ for the *decay* of the state with quantum numbers JMP. Thus it is assumed that $\mathfrak{M}_{JMP}$ can be written in a suitably Bose-symmetrized factorizable product form:

$$\mathfrak{M}_{JMP} = \sum_{LS} C^J_{LS}(W)[\mathfrak{R}_{LS}(s_1, W)Z^{JM}_{LS}(\Omega_1, \bar{\Omega}_1) + \mathfrak{R}_{LS}(s_2, W)Z^{JM}_{LS}(\Omega_2, \bar{\Omega}_2)]. \tag{4.2}$$

Here $C^J_{LS}(W)$ is independent of M and is a function

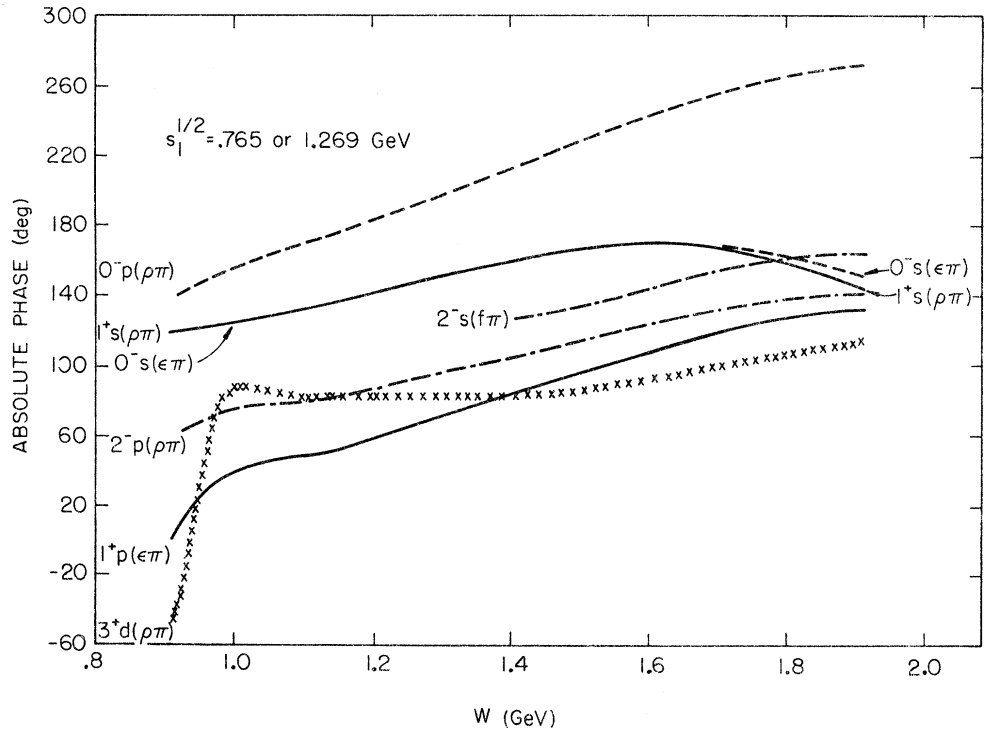

FIG. 14. Absolute phase of the important partial-wave amplitudes, as a function of 3π mass. Only the large amplitude $F_{++} + F_{--}$ is plotted. The dipion mass was set at 0.765 GeV for waves labeled $\rho\pi$ and $\epsilon\pi$, and 1.269 GeV for waves labeled $f\pi$. $P_{\text{lab}} = 16$ GeV, $t' = -0.05$ GeV.

only of the three-pion invariant mass W; $\mathcal{R}_{LS}(s_1, W)$ is independent of J and M and is a function of W and the dipion mass $\sqrt{s_1}$. As written in Eq. (4.2), it is assumed that the state with quantum numbers JMP decays coherently (like a resonant state with these quantum numbers). This assumption can be eliminated (at the expense of greatly increasing the number of parameters to be determined by the fit) by treating the states with different L, S separately, i.e., by transferring the $\sum_{LS}$ in (4.2) to (4.1) and using an enlarged density matrix $\rho_{JMPLS,J'M'P'L'S'}$.

In practice, L and S are restricted to low values ($S=0, 1, 2$; $L=0, 1, 2, 3$) and a Breit-Wigner form with appropriate threshold factors is used for $\mathcal{R}_{LS}(s_1, W)$:

$$\mathcal{R}_{LS}(s_1, W) = \frac{p_1^{\,L} q_1^{\,S}}{M_R^{\,2} - s_1 - iM_R\Gamma} . \tag{4.3}$$

$$\Gamma = \Gamma_R \left(\frac{q_1}{q_R}\right)^{2S+1} \frac{M_R}{\sqrt{s_1}} . \tag{4.4}$$

Here p_1 and q_1 are given by (2.22) and (2.23), and M_R and Γ_R are the mass and width of one or the other of the three well-known dipion resonances (see Table II). q_R in (4.4) is q_1 [Eq. (2.23)] evaluated at $s_1 = M_R^{\,2}$.

The formula (4.3) corresponds to a cascade decay process. The system first decays into a pion plus a dipion resonance of spin S. The Breit-Wigner denominator describes the propagation of the resonant state. Finally the dipion resonance decays into two pions. The threshold factors in the numerator are the simplest possible approximations to the matrix elements for the successive two-particle decay processes.

It is clear that these assumptions of the program

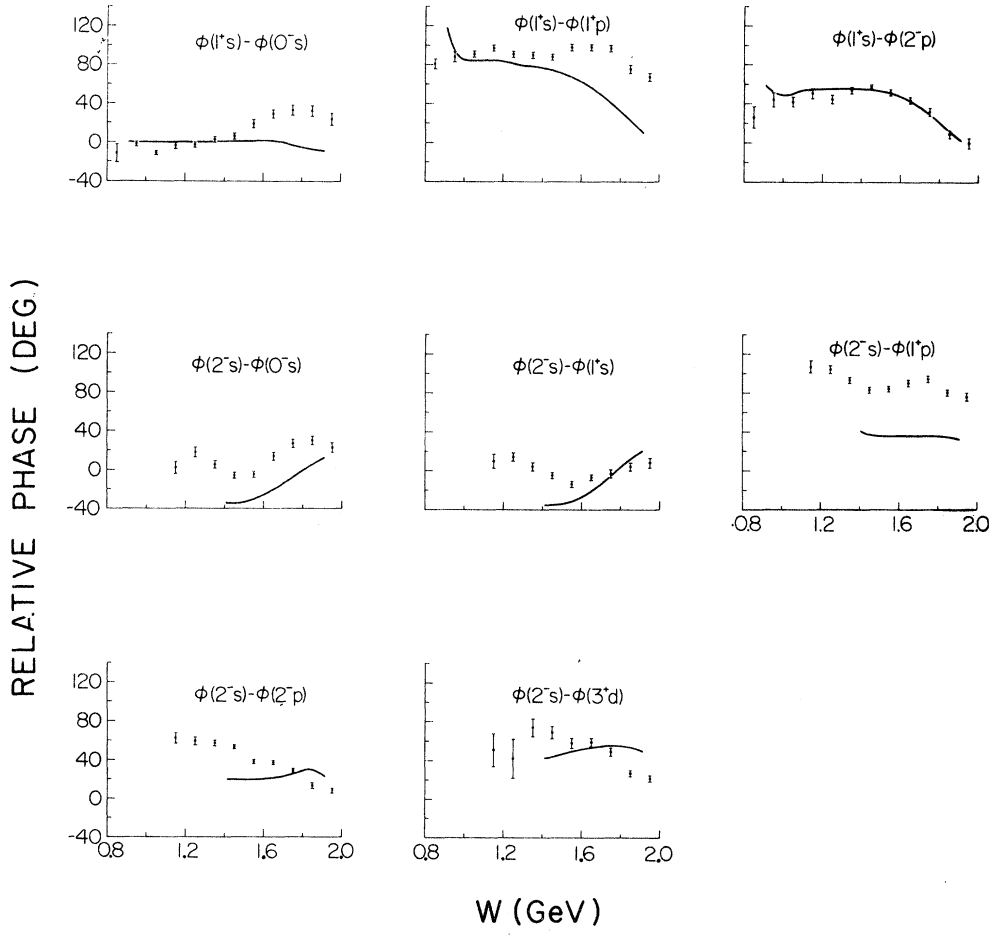

FIG. 15. Relative phases of the partial waves important in A_1 and A_3 regions. Solid lines indicate calculated values; points with error bars were obtained by applying the program FIT to a sample of Monte Carlo events.

TABLE II. Masses and widths used to parametrize $\pi\pi$ resonances in the program FIT.

	M_R	Γ_R
ϵ	0.765 GeV	0.400 GeV
ρ	0.765	0.135
f	1.269	0.154

FIT are not completely general, especially since in practice one severely restricts the number of allowed states in order to deal with a reasonable number of parameters $C_{LS}^{J}(W)$ and $\rho_{J'M'P',JMP}$ to be determined by the fitting procedure. It is equally clear that the Deck amplitude will not, in general, produce JMP states which decay in the fashion given by (4.2). In this section we (a) examine the partial-wave amplitudes calculated from the Deck model to see to what extent they have the properties assumed in Eq. (4.2), and (b) discuss the application of FIT to a sample of Monte Carlo events generated from the Deck amplitude to see whether the maximum-likelihood method can extract the correct partial-wave amplitudes in spite of the differences in form. We find that FIT does quite a good job, considering the differences between the Deck model and the assumed form.

A. Form of Amplitudes

From Eqs. (4.2) and (4.3) we see that as applied to the Deck model FIT in effect approximates $\pi\pi$ scattering by the form

$$\frac{{q_1}^S}{{M_R}^2 - s_1 - iM_R\Gamma}$$

and that after this "$\pi\pi$ amplitude" is removed, the only dependence of the partial waves on dipion mass s_1 lies in the threshold factor ${p_1}^L$. Plots of our amplitudes for fixed W as s_1 varies show that both the magnitude and the phase vary as s_1 varies, and the magnitude changes like ${p_1}^L$ only *extremely* near the threshold values. Hence the phases and magnitudes obtained for $C_{LS}^{J}(W)$ by fitting all events in one W bin are actually averages over s_1 of numbers which do vary with s_1.

How important is this variation? Most events will have $\sqrt{s_1}$ near the ρ, ϵ, or f mass; thus the neglected variation will be serious only if the amplitudes vary rapidly near these points. In Sec. III, we show Argand plots of some of the interesting amplitudes, with $\sqrt{s_1}$ fixed at values right on resonance and ±50 MeV from the resonance (Figs. 10 and 11). It can be seen that the variation with $\sqrt{s_1}$ is not rapid near these points and the averaging will not pose a great problem.

Since no experimental information is available about the nucleon spin structure in this amplitude, FIT neglects nucleon spin (and therefore is effectively using a spin-averaged amplitude in $\rho_{JMP,J'M'P'}$). This reduces the number of parameters, but it has the effect of assuming that the nucleon spin structure of states with identical JMP, but different L and S, is the same. A sampling of values for the $M=0$ amplitudes is enough to indicate that this assumption is not valid for the Deck model. However, as long as we are in a region where only one of the L, S states is dominant for a given J, M, P, this limitation of the parameters in FIT should probably not matter much. The determination of the sizes of the small states is not expected to be as accurate as that of the large states; this nucleon spin dependence will give one more reason for uncertainty in the small states.

Finally, the form of (4.2) indicates that the ratio of partial-wave amplitudes with the same JMP and different L and S should not depend on M. Again, this is not true in the Deck model. However, the dominance of $M=0$ in the model means that this defect of FIT should just show up in the sizes of the small states.

We conclude that the simple form of the gross features of the Deck model (dominance of $L=0$ and $M=0$) should minimize difficulties due to differences from the form assumed in FIT. However, the facts that (1) the ϵ effect in $\pi\pi$ scattering does not look exactly like a Breit-Wigner distribution at 765 MeV, (2) the program must average over s_1, and (3) the Deck model has a large tail of high-L partial waves which are not included in the fitting hypothesis, indicate that a fair amount of deviation between FIT and the calculated phases and magnitudes can be expected.

B. Comparison of Answers

In Figs. 8 and 15 we display the magnitudes and phases calculated by FIT as points with error bars, on the same plot as the curves found by explicit calculation with the formulas of Sec. II.

FIT does a fairly good job of extracting the total amounts of each JP state for the 0^-, 1^+, and 2^- states. The fitted values for the 1^+ and 2^- states are high at large W; this is to be expected because at large W many values of J are important in the Deck amplitude but FIT must absorb all events into the hypotheses available. The totals for the 3^+ state are uniformly high; again this is probably

because this state is acting as a "garbage collector."

If we turn our attention to the relative phases between the 1^+s state and other states that are large in the A_1 region, we see that FIT does a creditable job in the region up to $W = 1.4$ GeV, for all three states. It does an excellent job at all W for the $1^+s - 2^-p$ phase difference; both states in this difference are $\rho\pi$ states. The discrepancies between FIT and the calculated values for $\varphi_{1^+s} - \varphi_{0^-s}$ and $\varphi_{1^+s} - \varphi_{1^+p}$ when $W > 1.4$ GeV may therefore be attributed to treatment of the $\epsilon\pi$ states in 0^-s and 1^+p. This is probably caused by FIT's averaging over s_1, and the fact that there is a $\pi\pi$ s-wave effect near the f mass which will start contributing to the 3π spectrum near $W = 1.4$ GeV.

If we attribute the discrepancies between FIT and the calculation for $\varphi_{2^-s} - \varphi_{0^-s}$ and $\varphi_{2^-s} - \varphi_{1^+p}$ to this same effect, the remaining three phases in the A_3 region involve only $f\pi$ and $\rho\pi$ states. Both of these states are "cleaner" than the $\epsilon\pi$ state, as the ρ and f are the only well-documented $J = 1$ and 2 $\pi\pi$ resonances. The agreement between FIT and the calculation is quite reasonable for these states. The fact that in all three cases the FIT phases are slightly high at low W and slightly low at high W suggests that there are systematic effects due to the averaging by FIT in these cases also, but that they are not so severe.

These results give us (limited) confidence that the relative phases important for interpretation of the A_1 and A_3 effects can be extracted from data by FIT even for an amplitude as different from cascade decay as the one provided by Deck.

The magnitudes of particular L, S states are also reproduced reasonably well except for the $1^+s(\rho\pi)$ state near the A_1 peak. Here FIT produced a flatter peak than the calculation. To some extent this difficulty may be attributed to a remarkable similarity between the $1^+s(\rho\pi)$ and $1^+p(\epsilon\pi)$ states at low W,[14] which makes it hard for FIT to distinguish events belonging to the two states if $W < 1.2$ GeV. However, this cannot completely account for the flatness of the peak, for attempts to force FIT to follow the calculated curve decrease the likelihood by a substantial amount.

We conclude that FIT does a creditable job, considering the many differences between the form of the Deck model and the form assumed by FIT. Some of these differences could be removed by inserting actual $\pi\pi$ scattering amplitudes as part of the functions $\mathcal{R}_{LS}(s_1, W)$, and modifications of this sort might be considered for use of FIT in the future. However, we wanted to use exactly the same form of the program that has been used in fitting the data to facilitate comparison of the results.

V. SYMMETRY PROPERTIES OF DECK PARTIAL-WAVE AMPLITUDES

A. Consequences of Parity Invariance for $\pi N \to \pi\pi\pi N$

Helicity states have simple properties under reflection, or parity symmetry P.[15] In the rest frame of the 3π system, the incoming and outgoing nucleons lie in the xz plane. It is thus convenient to use reflection in this plane, $Y = e^{-i\pi J_y} P$, instead of the full parity operation. Using the relation

$$Y|J\lambda'\rangle = \eta(-1)^{J-\lambda'}|J-\lambda'\rangle, \tag{5.1}$$

valid for a particle moving in the xz plane, where J is the spin of the particle and η is its parity, we may construct states of definite Y for nucleons. The states $(1/\sqrt{2})(|\frac{1}{2}\frac{1}{2}\rangle \pm i|\frac{1}{2}-\frac{1}{2}\rangle)$ are eigenstates of Y with eigenvalues $\mp i$, respectively. The conjugate states $(1/\sqrt{2})(\langle\frac{1}{2}\frac{1}{2}| \mp i\langle\frac{1}{2}-\frac{1}{2}|)$ likewise have $Y^+ = \pm i$. The pion is an eigenstate of Y with eigenvalue -1. For simplicity in what follows, we will abbreviate the nucleon states as $(1/\sqrt{2})(|+\rangle \pm i|-\rangle)$, suppressing the explicit $S = \frac{1}{2}$.

Because the strong interactions conserve parity, matrix elements of the interaction taken between nucleon states of definite Y will vanish unless the three pions produced are also in an eigenstate of Y with the proper eigenvalue. In particular the 3π states produced by the amplitudes

$$\tfrac{1}{2}(\langle+|-i\langle-|)T(|+\rangle+i|-\rangle) = \tfrac{1}{2}(T_{++} + T_{--} - iT_{-+} + iT_{+-})$$

and

$$\tfrac{1}{2}(\langle+|+i\langle-|)T(|+\rangle-i|-\rangle) = \tfrac{1}{2}(T_{++} + T_{--} + iT_{-+} - iT_{+-})$$

must be eigenstates of Y with $Y = -1$; the 3π states produced by the amplitudes

$$\tfrac{1}{2}(\langle+|+i\langle-|)T(|+\rangle+i|-\rangle) = \tfrac{1}{2}(T_{++} - T_{--} + iT_{-+} + iT_{+-})$$

and

$$\tfrac{1}{2}(\langle+|-i\langle-|)T(|+\rangle-i|-\rangle) = \tfrac{1}{2}(T_{++} - T_{--} - iT_{-+} - iT_{+-})$$

must be eigenstates of Y with $Y = +1$. Adding and subtracting to obtain the amplitudes used in Sec. II, we find that $\frac{1}{2}(T_{++} + T_{--})$ and $\frac{1}{2}(T_{-+} - T_{+-})$ produce states of negative Y. Likewise $\frac{1}{2}(T_{++} - T_{--})$ and $\frac{1}{2}(T_{+-} + T_{-+})$ produce states of positive Y.

The three-pion states of definite Y are best catalogued using their quantum numbers J, M, and P. Since $Y|JM\rangle = P(-1)^{J-M}|J-M\rangle$, the combinations $|JM\rangle \pm P(-1)^{J-M}|J-M\rangle$ will be eigenstates of Y with $Y = \pm 1$, respectively. These will be produced in the amplitudes $\frac{1}{2}(T_{++} - T_{--})$ and $\frac{1}{2}(T_{-+} + T_{+-})$ (for $Y_{3\pi} = +1$), and $\frac{1}{2}(T_{++} + T_{--})$ and $\frac{1}{2}(T_{-+} - T_{+-})$ (for $Y_{3\pi} = -1$).

A considerable simplification results if $M = 0$, for in that case the state $|JM\rangle$ is itself an eigen-

state of Y with eigenvalue $P(-1)^J$. Thus $\frac{1}{2}(T_{++}+T_{--})$ and $\frac{1}{2}(T_{-+}-T_{+-})$ will produce 3π states with $M=0$ only if $P(-1)^J=-1$; and $\frac{1}{2}(T_{++}-T_{--})$ and $\frac{1}{2}(T_{-+}+T_{+-})$ will produce states with $M=0$ only if $P(-1)^J=+1$.

Corresponding results of parity invariance for our partial-wave amplitudes may be derived by examining the $2\to3$ reaction $\pi^-N\to(\pi^-\pi^+)_S\pi^-N$, where the dipion system is treated as a particle with mass $\sqrt{s_1}$ and spin S. In general, reactions of this type will have $4(2S+1)$ helicity amplitudes; in the 3π rest frame these amplitudes depend on the variables s, t, W, s_1, and the angles θ_1 and φ_1 of the dipion produced. We use the notation $f_{\lambda\lambda_2;\lambda_1}(s,t,W,s_1,\theta_1,\varphi_1)$ where λ_1 is the helicity of the incident nucleon, λ_2 is the helicity of the outgoing nucleon, and λ is the helicity of the outgoing $\pi^+\pi^-$ system.

Invariance under Y now tells us that

$$f_{\lambda\lambda_2;\lambda_1}(s,t,W,s_1,\theta_1,\varphi_1)=\eta_{2\pi}(-1)^{S-\lambda}(-1)^{\lambda_2-\lambda_1}\times f_{-\lambda-\lambda_2;-\lambda_1}(s,t,W,s_1,\theta_1,-\varphi_1).$$

Since the $\pi^+\pi^-$ system must have $\eta_{2\pi}=(-1)^S$, we arrive at the general parity relation

$$f_{\lambda\lambda_2;\lambda_1}(s,t,W,s_1,\theta_1,\varphi_1)=(-1)^{\lambda_2-\lambda_1-\lambda}\times f_{-\lambda-\lambda_2;-\lambda_1}(s,t,W,s_1,\theta_1,-\varphi_1). \tag{5.2}$$

We decompose our $2\to3$ amplitude into $2\to2$ partial waves for production of spin-J 3π states with spin projection M along the incident beam by [see Eq. (2.6)]

$$f_{\lambda\lambda_2;\lambda_1}=\sum_{JLM}F^{JM}_{LS;\lambda_2\lambda_1}\left(\frac{2L+1}{2J+1}\right)^{1/2}\langle J\lambda|LS0\lambda\rangle\times\left(\frac{2J+1}{4\pi}\right)^{1/2}\left(\frac{2S+1}{4\pi}\right)^{1/2}D^{J*}_{M\lambda}(\varphi_1,\theta_1,0). \tag{5.3}$$

The combinations $f_{\lambda\lambda_2;\lambda_1}\pm f_{\lambda-\lambda_2;-\lambda_1}$ then have partial-wave amplitudes $F^{JM}_{LS;\lambda_2\lambda_1}\pm F^{JM}_{LS;-\lambda_2-\lambda_1}$, which represent contributions to the $2\to2$ process $\pi N\to(3\pi)_{JM}N$:

$$F^{JM}_{LS;\lambda_2\lambda_1}\pm F^{JM}_{LS;-\lambda_2-\lambda_1}=\left(\frac{2L+1}{2S+1}\right)^{1/2}\sum_\lambda\langle J\lambda|LS0\lambda\rangle\int_0^{2\pi}d\varphi_1\int_{-1}^{1}d\cos\theta_1 D^J_{M\lambda}(\varphi_1,\theta_1,0)(f_{\lambda\lambda_2;\lambda_1}\pm f_{\lambda-\lambda_2;-\lambda_1}). \tag{5.4}$$

The general parity symmetry stated in Eq. (5.2) tells us that

$$F^{JM}_{LS;\lambda_2\lambda_1}=(-1)^{J_{3\pi}-L-S-M+\lambda_1-\lambda_2}F^{J-M}_{LS;-\lambda_2-\lambda_1}=-P_{3\pi}(-1)^{J_{3\pi}-M}(-1)^{\lambda_1-\lambda_2}F^{J-M}_{LS;-\lambda_2-\lambda_1}. \tag{5.5}$$

Hence

$$F^{JM}_{LS;\lambda_2\lambda_1}\pm(-1)^{\lambda_1-\lambda_2}F^{JM}_{LS;-\lambda_2-\lambda_1}=F^{JM}_{LS;\lambda_2\lambda_1}\mp P_{3\pi}(-1)^{J_{3\pi}-M}F^{J-M}_{LS;\lambda_2\lambda_1}$$

and the $f_{\lambda+;+}+f_{\lambda-;-}$ and $f_{\lambda+;-}-f_{\lambda-;+}$ amplitudes couple to three-pion states $|JM\rangle-P_{3\pi}(-1)^{J_{3\pi}-M}|J-M\rangle$, whereas the $f_{\lambda+;+}-f_{\lambda-;-}$ and $f_{\lambda+;-}+f_{\lambda-;+}$ amplitudes couple to three-pion states $|JM\rangle+P_{3\pi}(-1)^{J_{3\pi}-M}\times|J-M\rangle$ as demonstrated in a different manner above.

For the nucleons, states of definite Y are states with definite spin projection along the y axis. This may be seen simply by constructing states $(1/\sqrt{2})(\frac{1}{\pm i})$ of definite J_y from states of definite z component of spin. If we rotate about the y axis from the z direction to the nucleon direction these states are acted upon by $e^{-iJ_y\theta_i}$, which just leads to a multiplicative phase factor (since they are eigenstates of J_y). Hence the helicity combinations $(1/\sqrt{2})(|+\rangle\pm i|-\rangle)$ are eigenstates of σ_y with eigenvalues ±1.

This fact leads to a great simplification for Lorentz transformations of the system which keep the nucleon momentum vectors in the xz plane. Such Lorentz transformations act on the nucleon spin like rotations about the y axis, $|\frac{1}{2}\lambda\rangle\to e^{-iJ_y\xi}\times|\frac{1}{2}\lambda\rangle$. Hence our amplitudes producing 3π states with $Y=-1$ transform to

$$\tfrac{1}{2}(\langle+|\mp i\langle-|)e^{iJ_y\xi_2}Te^{-iJ_y\xi_1}(|+\rangle\pm i|-\rangle)=e^{\mp i\xi_1/2\pm i\xi_2/2}\tfrac{1}{2}(\langle+|\mp i\langle-|)T(|+\rangle\pm i|-\rangle) \tag{5.6}$$

and our amplitudes producing 3π states with $Y=+1$ transform to

$$\tfrac{1}{2}(\langle+|\pm i\langle-|)e^{iJ_y\xi_2}Te^{-iJ_y\xi_1}(|+\rangle\pm i|-\rangle)=e^{\mp i\xi_1/2\mp i\xi_2/2}\tfrac{1}{2}(\langle+|\pm i\langle-|)T(|+\rangle\pm i|-\rangle). \tag{5.7}$$

We see that no matter what the Lorentz transfor-

mation in the xz plane, there will be two classes of amplitudes which mix among themselves but not with members of the other class. Using helicity-labeled amplitudes, we see that $T_{++}+T_{--}$ and $T_{+-}-T_{-+}$ will mix with an angle $\frac{1}{2}(\xi_1-\xi_2)$, whereas $T_{++}-T_{--}$ and $T_{+-}+T_{-+}$ will mix with an angle $\frac{1}{2}(\xi_1+\xi_2)$. As it is convenient to transform from the 3π rest frame to the lab frame, to the t-channel center-of-mass frame, and to the s-channel center-of-mass frame (all of which involve spin rotation around the y axis), we will find this useful.

As an example of this, let us relate our amplitudes, calculated in the s-channel rest frame of the 3π system, to those in the t-channel center-of-mass for $\bar{N}N\to(3\pi)\pi$. We begin by using the arguments of Trueman and Wick[16] to relate our s-channel 3π rest-frame amplitudes $f_{M\mu;0\lambda}$ to the corresponding t-channel 3π rest-frame amplitudes $g_{M0;\mu\lambda}$. We find (up to an over-all phase) that

$$f_{M\mu;0\lambda}(q_2,-p_2;-q_1p_1)=g_{M0;\mu\lambda}(q_2,q_1;p_2,p_1)\,. \quad (5.8)$$

Next we must rotate the nucleon spins from the 3π rest frame to the t-channel center-of-mass rest frame. The 3π spin projection M will not change since it is along the same direction (the pion direction) in each case.

$$g_{M0;ij}=\sum_{i'j'} d^{1/2}_{ii'}(\xi_1)d^{1/2}_{jj'}(\xi_2)f^t_{M0;i'j'}\,, \quad (5.9)$$

where

$$\cos\xi_2=\frac{+t(s+t-m_p{}^2-m_\pi{}^2)-2m_p{}^2(t-m_\pi{}^2+W^2)}{2W\sqrt{t}\,(t-4m_p{}^2)^{1/2}(E_B{}^2-m_p{}^2)^{1/2}}$$

and

$$\cos\xi_1=\frac{-t(s-W^2-m_p{}^2)-2m_p{}^2(t-m_\pi{}^2+W^2)}{2W\sqrt{t}\,(t-4m_p{}^2)^{1/2}(E_D{}^2-m_p{}^2)^{1/2}}\,,$$

with E_B and E_D defined in Eq. (2.30).

Writing out Eq. (5.9) and using the relations between d functions, we find that

$$f_{M+;0+}+f_{M-;0-}=(f^t_{M0;++}+f^t_{M0;--})\cos\tfrac{1}{2}(\xi_1-\xi_2)+(f^t_{M0;+-}-f^t_{M0;-+})\sin\tfrac{1}{2}(\xi_1-\xi_2)\,, \quad (5.10a)$$

$$f_{M+;0-}-f_{M-;0+}=-(f^t_{M0;++}+f^t_{M0;--})\sin\tfrac{1}{2}(\xi_1-\xi_2)+(f^t_{M0;+-}-f^t_{M0;-+})\cos\tfrac{1}{2}(\xi_1-\xi_2)\,, \quad (5.10b)$$

$$f_{M+;0+}-f_{M-;0-}=(f^t_{M0;++}-f^t_{M0;--})\cos\tfrac{1}{2}(\xi_1+\xi_2)-(f^t_{M0;+-}+f^t_{M0;-+})\sin\tfrac{1}{2}(\xi_1+\xi_2)\,, \quad (5.11a)$$

$$f_{M+;0-}+f_{M-;0+}=(f^t_{M0;++}-f^t_{M0;--})\sin\tfrac{1}{2}(\xi_1+\xi_2)+(f^t_{M0;+-}+f^t_{M0;-+})\cos\tfrac{1}{2}(\xi_1+\xi_2)\,, \quad (5.11b)$$

which shows explicitly that the $|++\rangle+|--\rangle$ and $|+-\rangle-|-+\rangle$ combinations are rotated by $\frac{1}{2}(\xi_1-\xi_2)$, while the $|++\rangle-|--\rangle$ and $|+-\rangle+|-+\rangle$ combinations are rotated by $\frac{1}{2}(\xi_1+\xi_2)$.

B. Simplifications in Our Model Due to the Form of Couplings Chosen for the Exchanged Pion

Although we have Reggeized the exchanged pion, we have kept the couplings the same as those for an elementary pion. This places constraints on the form of the amplitude, because the spin-zero elementary pion has only one form of coupling. These constraints provide us with a model with some special properties. In particular, (i) amplitudes for production of 3π states with $Y=\pm1$ are odd or even, respectively, under the replacement $\varphi\to-\varphi$, and (ii) only natural parity is exchanged in the $N\bar{N}$ vertex in the t channel. This reduces the number of independent amplitudes. We will consider (i) and (ii) in turn.

Evenness or Oddness in φ

Because our dipion is produced from an incident pion beam with an exchange coupling like an elementary pion, the dipion has spin component zero along the incident beam in the dipion rest frame. The various amounts of different helicities λ are produced as we see for example from Eq. (2.12) by a rotation into the 3π rest frame, $d^s_{0\lambda}(\psi)$ with $\tan\psi$ given by Eq. (2.30). Notice that rotation through ψ produces no φ dependence. Hence the dependence on φ of the amplitudes in our model is not connected with the dipion end of the graph; it is all at the πN scattering end of the graph and is not related to the dipion helicity. In effect, therefore, the helicity amplitudes take the form

$$f_{\lambda\lambda_2;\lambda_1}(s,t_{NN},W,s_1,\theta_1,\varphi_1)=d^s_{0\lambda}(\psi)g_{\lambda_2\lambda_1}(s,t_{NN},W,s_1,\theta_1,\varphi_1)\,.$$

This follows directly from substitution of Eq. (2.8) into Eq. (2.7). Our parity relation Eq. (5.2) then leads to

$$g_{\lambda_2\lambda_1}(s,t_{NN},W,s_1,\theta_1,\varphi_1)=(-1)^{\lambda_2-\lambda_1}g_{-\lambda_2-\lambda_1}(s,t_{NN},W,s_1,\theta_1,-\varphi_1)\,.$$

Hence we finally arrive at

$$f_{\lambda\lambda_2;\lambda_1}(s,t,W,s_1,\theta_1,\varphi_1)=(-1)^{\lambda_2-\lambda_1}f_{\lambda-\lambda_2;-\lambda_1}(s,t,W,s_1,\theta_1,-\varphi_1)\,, \quad (5.12)$$

an equation special to our model.

The combinations $f_{\lambda+;+}(\theta_1,\varphi_1)+f_{\lambda-;-}(\theta_1,\varphi_1)$ and

$f_{\lambda+;-}(\theta_1,\varphi_1)-f_{\lambda-;+}(\theta_1,\varphi_1)$ are thus even in φ, and $f_{\lambda+;+}(\theta_1,\varphi_1)-f_{\lambda-;-}(\theta_1,\varphi_1)$ and $f_{\lambda+;-}(\theta_1,\varphi_1)+f_{\lambda-;+}(\theta_1,\varphi_1)$ are odd in φ, as was shown in Sec. II C using the explicit form of the amplitude with the $\pi\pi$ scattering removed.

t-Channel Quantum Numbers

By assuming that the exchanged pion couples like an elementary pion, we were able to put in on-shell πN scattering as one vertex. Pion-nucleon scattering has only natural parity exchange $[P_{ex}=(-1)^{J_{ex}}]$; hence our model will exhibit some additional symmetries.

The t-channel $(\pi,3\pi)$ states with total spin J_{ex}, 3π spin projection M, and parity $P_{ex}=(-1)^{J_{ex}}$, are $|J_{ex}M\rangle - P(-1)^J|J_{ex}-M\rangle$. Hence our t-channel partial-wave amplitudes obey the relation

$$T^{J_{ex}}_{M0;\lambda_1\lambda_2}(t)=-P(-1)^J T^{J_{ex}}_{-M0;\lambda_1\lambda_2}(t)\,. \tag{5.13}$$

Likewise, eigenstates of parity at the $N\bar{N}$ vertex with $P_{ex}=(-1)^{J_{ex}}$ are $|J_{ex}+\frac{1}{2}\pm\frac{1}{2}\rangle+|J_{ex}-\frac{1}{2}\mp\frac{1}{2}\rangle$, so we obtain an additional relation for the partial-wave amplitudes:

$$T^{J_{ex}}_{M0;\lambda_1\lambda_2}(t)=T^{J_{ex}}_{M0;-\lambda_1-\lambda_2}(t)\,. \tag{5.14}$$

These relations between partial waves make certain amplitudes vanish. From Eq. (5.13) we see that $T^{J_{ex}}_{00;\lambda_1\lambda_2}=0$ if $P=(-1)^J$. In subsection A of this section we demonstrated that the 3π rest-frame amplitudes $T_{++}-T_{--}$ and $T_{-+}+T_{+-}$ will produce 3π states with $M=0$ only if $P=(-1)^J$. Hence $T_{++}-T_{--}$ and $T_{-+}+T_{+-}$ will not contribute to any $M=0$ states in the model.

The other relation, Eq. (5.14), leads to

$$\begin{aligned} f^t_{M0;++}\pm f^t_{M0;--}&=\sum(2J_{ex}+1)(T^{J_{ex}}_{M0;++}\pm T^{J_{ex}}_{M0;--})d^{J_{ex}}_{0M}(\theta_t)\\ &=\begin{cases}2\sum(2J_{ex}+1)T^{J_{ex}}_{M0;++}d^{J_{ex}}_{0M}(\theta_t)\\ 0\,,\end{cases}\end{aligned} \tag{5.15}$$

$$\begin{aligned} f^t_{M0;+-}\pm f^t_{M0;-+}&=\sum(2J_{ex}+1)[T^{J_{ex}}_{M0;+-}d^{J_{ex}}_{1M}(\theta_t)\\ &\qquad\pm T^{J_{ex}}_{M0;-+}d^{J_{ex}}_{-1M}(\theta_t)]\\ &=\sum(2J_{ex}+1)T^{J_{ex}}_{M0;+-}[d^{J_{ex}}_{1M}(\theta_t)\\ &\qquad\pm d^{J_{ex}}_{-1M}(\theta_t)]\,.\end{aligned} \tag{5.16}$$

Since $d^{J_{ex}}_{1M}(\theta_t)-d^{J_{ex}}_{-1M}(\theta_t)$ is a power of $\cos\theta_t$ larger than $d^{J_{ex}}_{1M}(\theta_t)+d^{J_{ex}}_{-1M}(\theta_t)$ in the limit of large $\cos\theta_t$, we expect $f^t_{M0;+-}-f^t_{M0;-+}$ to dominate $f^t_{M0;-+}+f^t_{M0;-+}$ in the Regge limit (by a power of $\cos\theta_t$). Thus natural-parity exchange leads to the vanishing of one t-channel amplitude and the relative unimportance of another at large s. The two remaining large amplitudes are $f^t_{M0;++}+f^t_{M0;--}$ and $f^t_{M0;+-}-f^t_{M0;-+}$, which we saw previously produce 3π states of $Y=-1$.

The results derived here may be considered a special case of a general "theorem." In the case of a t-channel exchange of definite naturality $\sigma=P_{ex}(-1)^{J_{ex}}$ for the t-channel reaction $\bar{3}+4\to\bar{2}+1$, the combination of amplitudes $f^t_{\lambda_1\lambda_2;\lambda_3\lambda_4}+\sigma\eta f^t_{\lambda_1\lambda_2;-\lambda_3-\lambda_4}$ always dominates over $f^t_{\lambda_1\lambda_2;\lambda_3\lambda_4}-\sigma\eta f^t_{\lambda_1\lambda_2;-\lambda_3-\lambda_4}$ by a power of $\cos\theta_t$, and more specifically

$$\frac{f^t_{\lambda_1\lambda_2;\lambda_3\lambda_4}-\sigma\eta f^t_{\lambda_1\lambda_2;-\lambda_3-\lambda_4}}{f^t_{\lambda_1\lambda_2;\lambda_3\lambda_4}+\sigma\eta f^t_{\lambda_1\lambda_2;-\lambda_3-\lambda_4}}\underset{\cos\theta_t\to\infty}{\propto}\frac{(\lambda_1-\lambda_2)(\lambda_3-\lambda_4)}{\cos\theta_t}\,. \tag{5.17}$$

Here η is defined by the equation $Y|\lambda_3\lambda_4\rangle=\eta|-\lambda_3-\lambda_4\rangle$, or $\eta=\eta_3\eta_4(-1)^{J_3-\lambda_3+J_4+\lambda_4}$. The proof of this well-known "theorem," which follows from standard Regge arguments, is summarized for the convenience of the reader in an appendix. Here we merely note that for our case, $\sigma=+1$, and we have

$$\begin{aligned}&\frac{f^t_{\lambda_1\lambda_2;++}-f^t_{\lambda_1\lambda_2;--}}{f^t_{\lambda_1\lambda_2;++}+f^t_{\lambda_1\lambda_2;--}}\propto 0\,,\\ &\frac{f^t_{\lambda_1\lambda_2;+-}+f^t_{\lambda_1\lambda_2;-+}}{f^t_{\lambda_1\lambda_2;+-}-f^t_{\lambda_1\lambda_2;-+}}\propto\frac{\lambda_1-\lambda_2}{\cos\theta_t}\,,\end{aligned} \tag{5.18}$$

as shown specifically above.

Explicit Form of the t-Channel Helicity Amplitudes

In some of the discussion in subsequent parts of this section we will use the explicit form of the t-channel amplitudes in our model. As the amplitudes are relatively simple and exhibit the behavior expected from Eq. (5.18) in a pleasingly transparent fashion, we take the time to derive them here.

Straightforward insertion of spinors into our amplitude leads to the following t-channel results, where the pion propagator and $\pi\pi$ scattering amplitude have been omitted for convenience:

$$\begin{aligned} f^t_{++}+f^t_{--}&=-2\left(\mathfrak{A}\frac{p}{m_p}+\mathfrak{B}q_z\right),\\ f^t_{++}-f^t_{--}&=0\,,\\ f^t_{+-}-f^t_{-+}&=-2q_x\frac{E}{m_p}\mathfrak{B}\,,\\ f^t_{+-}+f^t_{-+}&=2iq_y\frac{E}{m_p}\mathfrak{B}\,.\end{aligned} \tag{5.19}$$

In Eq. (5.19) $\mathfrak{A}$ and $\mathfrak{B}$ are the invariant amplitudes from pion-nucleon scattering, $p=\frac{1}{2}(t-4m_p^2)^{1/2}$ and $E=\frac{1}{2}\sqrt{t}$ are the momentum and energy of the

nucleon in the t-channel center-of-mass system, and q_x, q_y, and q_z are the components of the momentum of the "bachelor" pion (the one not in a dipion resonance) in this frame. We have defined the z axis in this frame to be along the direction of the nucleon.

To cast this into a form where we can compare with the results derived above, the components q_i need to be reexpressed in a way such that the helicity states of the three-pion system can be picked off. Following our usual procedure, we first write the four-momentum of the bachelor pion in the t-channel rest frame of the three-pion system, using the incident pion beam in the t channel as a z' axis: $(E_1, q_1\sin\theta\cos\varphi, q_1\sin\theta\sin\varphi, q_1\cos\theta)$, where

$$E_1 = (W^2 + m_\pi{}^2 - s_1)/2W ,$$
$$q_1 = (E_1{}^2 - m_\pi{}^2)^{1/2} .$$

To get from the rest frame of the three-pion system to the t-channel center-of-mass system, we boost along this z' axis in the negative z' direction until the three-pion system acquires momentum

$$\frac{\{[t-(W-m_\pi)^2][t-(W+m_\pi)^2]\}^{1/2}}{2\sqrt{t}} = \beta W .$$

Defining $\gamma = (t + W^2 - m_\pi{}^2)/2\sqrt{t}\,W)$, our bachelor pion now has momentum

$$(E_1\gamma - \beta q_1\cos\theta, q_1\sin\theta\cos\varphi, q_1\sin\theta\sin\varphi, q_1\cos\theta\gamma - \beta E_1)$$

in the t-channel center-of-mass frame where the z' axis is given by the direction of the pion beam.

Finally, we must reexpress this in terms of the xyz axes determined by the t-channel nucleon. The scattering angle in the t channel in our convention is the angle between the nucleon and the incident pion; hence we need only rotate through θ_t to obtain the four-momentum needed in Eq. (5.19):

$$\begin{aligned}
\omega &= E_1\gamma - \beta q_1\cos\theta ,\\
q_x &= q_1\sin\theta\cos\varphi\cos\theta_t + \sin\theta_t(q_1\cos\theta\gamma - \beta E_1) ,\\
q_y &= q_1\sin\theta\sin\varphi ,\\
q_z &= (q_1\cos\theta\gamma - \beta E_1)\cos\theta_t - q_1\sin\theta\cos\varphi\sin\theta_t .
\end{aligned} \tag{5.20}$$

Using these components and the momentum vector $(E, 0, 0, -p)$ of the antinucleon in the t channel (which is the outgoing nucleon in the s channel), we can calculate $s_{\pi N}$, which appears in $\mathfrak{A}$ and $\mathfrak{B}$:

$$\begin{aligned}
s_{\pi N} = m_\pi{}^2 + m_p{}^2 &- 2E(E_1\gamma - \beta q_1\cos\theta)\\
&- 2p[(q_1\cos\theta\gamma - \beta E_1)\cos\theta_t\\
&\quad - q_1\sin\theta\cos\varphi\sin\theta_t] .
\end{aligned}$$

Notice that this is a function only of $\cos\varphi$.

Substituting into Eq. (5.19) we see immediately that

(i) $f^t_{+-} + f^t_{-+}$ is lower than $f^t_{+-} - f^t_{-+}$ by the expected power of $\cos\theta_t$ at large $\cos\theta_t$;

(ii) since $f^t_{+-} + f^t_{-+}$ is odd in φ, it can have no $M = 0$ pieces; and

(iii) *a priori* $f^t_{++} + f^t_{--}$ and $f^t_{+-} - f^t_{-+}$ are of the same order of magnitude.

C. High-Energy Behavior and Consequences of Helicity Conservation in πN Scattering

As was remarked in subsection B of this section, the two amplitudes $f^t_{++} + f^t_{--}$ and $f^t_{+-} - f^t_{-+}$, which produce three-pion states of $Y = -1$, are in general of similar size at high energy. In the event that pion-nucleon scattering exhibits helicity conservation (as it does in the amplitudes inserted for our numerical calculation), the invariant amplitudes $\mathfrak{A}$ and $\mathfrak{B}$ have the same order of magnitude at large energy. Since the $\mathfrak{B}$ terms in (5.19) are multiplied by additional factors of $\cos\theta_t$ and $\sin\theta_t$ from the q_i, we see that they will be the dominant contributors to our two dominant amplitudes.

From the discussion in Sec. V A, we realize that any Lorentz transformation in the scattering plane will result in a mixing of these two amplitudes which takes exactly the form of a rotation,

$$\begin{aligned}
(\text{New})_1 &= \cos\tfrac{1}{2}\varphi'(f^t_{++} + f^t_{--}) + \sin\tfrac{1}{2}\varphi'(f^t_{+-} - f^t_{-+}) ,\\
(\text{New})_2 &= -\tfrac{1}{2}\sin\varphi'(f^t_{++} + f^t_{--}) + \cos\tfrac{1}{2}\varphi'(f^t_{+-} - f^t_{-+}) ,
\end{aligned} \tag{5.21}$$

for an angle φ' which is the difference in angles of rotation for the two nucleon spins. Since the dominant piece of both amplitudes is proportional to $\mathfrak{B}$, we are tempted to try to cancel it off by performing a suitable rotation. This would lead us to a frame in which only one amplitude was dominant at high energy.

Beginning with the explicit forms of the two amplitudes of interest,

$$\begin{aligned}
f^t_{++} + f^t_{--} &= -2\left\{\mathfrak{A}\frac{p}{m_p} + \mathfrak{B}[(q_1\cos\theta\gamma - \beta E_1)\cos\theta_t\right.\\
&\qquad \left. - q_1\sin\theta\cos\varphi\sin\theta_t]\right\} ,\\
f^t_{+-} - f^t_{-+} &= -2\frac{E}{m_p}\mathfrak{B}[q_1\sin\theta\cos\varphi\cos\theta_t\\
&\qquad + \sin\theta_t(q_1\cos\theta\gamma - \beta E_1)] ,
\end{aligned}$$

we see that a rotation with

$$\begin{aligned}
\cos\tfrac{1}{2}\varphi' &= \frac{m_p\cos\theta_t}{[m_p{}^2 + (E^2 - m_p{}^2)\sin^2\theta_t]^{1/2}}\\
&= \frac{m_p\cos\theta_t}{D} ,
\end{aligned}$$

$$\sin\tfrac{1}{2}\varphi' = \frac{E\sin\theta_t}{[m_p^2+(E^2-m_p^2)\sin^2\theta_t]^{1/2}} = \frac{E\sin\theta_t}{D}$$

leads to

$$D(\text{New})_1 = -2\mathcal{A}p\cos\theta_t - \frac{2\mathcal{B}}{m_p}(q_1\cos\theta\gamma - \beta E_1)D^2 + \frac{2\mathcal{B}}{m_p}\cos\theta_t\sin\theta_t q_1(m_p^2-E^2)\sin\theta\cos\varphi, \tag{5.22}$$

$$D(\text{New})_2 = 2\mathcal{A}\frac{p}{m_p}E\sin\theta_t - 2\mathcal{B}q_1E\sin\theta\cos\varphi.$$

In this new frame, then, the amplitude $(\text{New})_1$ dominates at large energy, and the contribution of the $\mathcal{B}$ amplitude to $(\text{New})_2$ is of order $1/s$.

In the limit as $s\to\infty$,

$$\cos\tfrac{1}{2}\varphi' \to \frac{2m_p}{(4m_p^2-t)^{1/2}}, \qquad \sin\tfrac{1}{2}\varphi' \to \left(\frac{-t}{4m_p^2-t}\right)^{1/2}. \tag{5.23}$$

Examination of the rotation to the 3π rest frame given by (5.9) shows that in this limit

$$\cos\tfrac{1}{2}(\xi_1-\xi_2)\to\frac{2m_p}{(4m_p^2-t)^{1/2}}, \qquad \sin\tfrac{1}{2}(\xi_1-\xi_2)\to\left(\frac{-t}{4m_p^2-t}\right)^{1/2}$$

also. Hence the two rotations are the same at large s, thus proving that at large s our 3π rest-frame amplitudes behave like (5.22), i.e., $f_{++}+f_{--}\sim s$ and $f_{+-}-f_{-+}\sim$const at $t=0$.

These statements all assume that the large-s behavior of our partial-wave amplitudes may be obtained by examining the large $s_{\pi N}$ behavior of A and B. This of course, is only an approximation, since in obtaining the partial-wave amplitudes we integrate over all $\cos\theta_1$ at a given s, and thus actually include quite low $s_{\pi N}$ in the calculation. However, at very large energies, most of the region of θ_1 integration has large $s_{\pi N}$, so thinking in terms of the large energy behavior of $\mathcal{A}$ and $\mathcal{B}$ is a fairly good assumption.

Since this is the case, we can profitably use the concept of Pomeranchon exchange. If we assume a factorizing Pomeranchon exchange dominates the high-energy behavior of both $\pi N\to\pi N$ and $\pi N\to(3\pi)_{Y=-1}N$, then the residues at the nucleon vertex must obey

$$-\beta_{++}(t)\left(\frac{-t}{4m_p^2-t}\right)^{1/2}+\beta_{+-}(t)\frac{2m_p}{(4m_p^2-t)^{1/2}}=0 \tag{5.24}$$

in order that πN scattering preserve s-channel helicity at high energy. Insertion of the high-energy behavior of $\cos\frac{1}{2}(\xi_1-\xi_2)$ and $\sin\frac{1}{2}(\xi_1-\xi_2)$ into Eq. (5.10b) shows that because of (5.24) our 3π rest frame amplitude $f_{+-}-f_{-+}$ will be down by a power of s from $f_{++}+f_{--}$. Hence the behavior detailed in Eq. (2.32) can be entirely explained in terms of Regge language.

We note also that the transformation from the t-channel rest frame to the s-channel rest frame is given by the following nucleon rotation angles:

$$\cos\theta_1=\frac{-\sqrt{t}\,(s+m_p^2-m_{3\pi}^2)-2m_p^2(W^2-m_\pi^2)/\sqrt{t}}{(t-4m_p^2)^{1/2}\delta_{N,3\pi}},$$

$$\cos\theta_2=\frac{\sqrt{t}\,(s+m_p^2-m_\pi^2)-2m_p^2(W^2-m_\pi^2)/\sqrt{t}}{(t-4m_p^2)^{1/2}\delta_{N,\pi}},$$

where $\delta_{ab}=([s-(M_a-M_b)^2][s-(M_a+M_b)^2])^{1/2}$. At large s this gives the same rotation, with $\cos\frac{1}{2}(\theta_1-\theta_2)=2m_p/(4m_p^2-t)^{1/2}$. Hence direct-channel helicity conservation for πN scattering gives approximate s-channel helicity conservation at the nucleon vertex in our reaction also. We have previously seen that $M=0$ dominates in the produced 3π states. Hence we have a model with approximate s-channel helicity conservation at the nucleon vertex but approximate t-channel helicity conservation at the meson vertex.

The similarity of all these transformations [the one to the "new" frame given by (5.22), the one to the s-channel center-of-mass frame, and the one to the s-channel 3π rest frame] is not, of course, a coincidence. The angles for nucleon rotation in all such transformations take the form

$$\cos\theta_1=\frac{-\sqrt{t}\,E_1-2m_p^2\gamma_{\text{trans}}}{(t-4m_p^2)^{1/2}p_1},$$

$$\cos\theta_2=\frac{\sqrt{t}\,E_2-2m_p^2\gamma_{\text{trans}}}{(t-4m_p^2)^{1/2}p_2},$$

where E_i, P_i are the resulting energies and momenta and $\gamma_{\text{trans}}=(E_2-E_1)/\sqrt{t}$ is the parameter characterizing the over-all transformation from the t-channel center-of-mass frame. Hence any frame with $E_2, E_1\to\infty$, and $E_2-E_1\to$ const (where the constant may be zero) as $s\to\infty$ will yield a set of amplitudes identical in nucleon spin structure to our 3π rest-frame amplitudes in the large-energy limit.

D. Further Comments About Dependence of Our Calculation on the πN Helicity-Conserving Amplitude

Because our calculation required πN scattering amplitudes from threshold to large energies, we used phase shift and Regge information in their respective regions of relevance. Unfortunately, as discussed above, amplitudes calculated from phase shifts do not exactly match onto those from Regge formulas. We settled for a linear interpolation between the two formulas in the region

$2 \leq (s_{\pi N})^{1/2} \leq 2.2$ GeV. This is not a bad approximation for the helicity-conserving amplitude, where the discontinuity between Regge and phase shifts is slight, but it is more drastic for $\mathcal{A}$ and $\mathcal{B}$ individually (especially $\mathcal{A}$) at most values of momentum transfer.

Hence the credibility of our results depends to some extent on the degree in which our amplitude is a function only of the πN helicity conserving amplitude. In this section we show explicitly that the ratio of the large amplitude $(\text{New})_1$ derived in Eq. (5.22) to the πN helicity-preserving amplitude approaches 1 as $s \to \infty$.

We begin with the formula

$$(\text{New})_1 = -2\mathcal{A}_p \frac{\cos\theta_t}{D} - \frac{2\mathcal{B}}{m_p}(q_1\cos\theta\gamma - \beta E_1)D + \frac{2\mathcal{B}}{m_p}\cos\theta_t \frac{\sin\theta_t}{D} q_1(m_p^2 - E^2)\sin\theta\cos\varphi$$

and the algebraically useful exact expressions

$$D/\cos\theta_t = \tfrac{1}{2}(4m_p^2 - t)^{1/2}\left(1 - \frac{\tau_{\pi,3\pi}^2}{(s-u)^2}\right)^{1/2},$$

$$D = \frac{\sqrt{-t}\,(s-u)}{2\tau_{\pi,3\pi}}\left(1 - \frac{\tau_{\pi,3\pi}^2}{(s-u)^2}\right)^{1/2},$$

$$\sin\theta_t = \left(\frac{-t}{t}\right)^{1/2}\frac{(s-u)}{\tau_{\pi,3\pi}} \times\left[\left(-t - \frac{(4m_p^2 - t)\tau_{\pi,3\pi}^2}{(s-u)^2}\right)^{1/2}\right]\Big/(4m_p^2 - t)^{1/2},$$

where $\tau_{\pi,3\pi}^2 = [t - (W - m_\pi)^2][t - (W + m_\pi)^2]$. Hence the amplitude is

$$\frac{-2\mathcal{A}(t - 4m_p^2)^{1/2}}{(4m_p^2 - t)^{1/2}[1 - \tau_{\pi,3\pi}^2/(s-u)^2]^{1/2}} - \frac{\mathcal{B}}{m_p}(q_1\cos\theta\gamma - \beta E_1)\cos\theta_t(4m_p^2 - t)^{1/2}\left(1 - \frac{\tau_{\pi,3\pi}^2}{(s-u)^2}\right)^{1/2} + \frac{4\mathcal{B}}{m_p}q_1\frac{(m_p^2 - E^2)\sin\theta\cos\varphi\sin\theta_t}{(4m_p^2 - t)^{1/2}[1 - \tau_{\pi,3\pi}^2/(s-u)^2]^{1/2}}. \quad (5.25)$$

As $s \to \infty$, $[1 - \tau_{\pi,3\pi}^2/(s-u)^2]^{1/2} \to 1$ to order $1/s^2$ and we obtain

$$-\frac{(t - 4m_p^2)^{1/2}}{(4m_p^2 - t)^{1/2}}\left[2\mathcal{A} - \frac{2\mathcal{B}}{m_p}p\cos\theta_t(q_1\cos\theta\gamma - \beta E_1) + \frac{2\mathcal{B}}{m_p}q_1 p\sin\theta\cos\varphi\sin\theta_t\right].$$

The πN helicity-conserving amplitude takes the form $2\mathcal{A} - (2\mathcal{B}/m_p)q_\pi \cdot p_D$ (after removal of a kinematic factor containing $\cos\frac{1}{2}\theta$). In our frame

$$q_\pi \cdot p_D = E(E_1\gamma - \beta q_1\cos\theta) + p(q_1\cos\theta\gamma - \beta E_1)\cos\theta_t - pq_1\sin\theta\cos\varphi\sin\theta_t.$$

Hence the πN helicity-conserving (h.c.) amplitude as used in our model is

$$2\mathcal{A} - \frac{2\mathcal{B}}{m_p}\{E(E_1\gamma - \beta q_1\cos\theta) + p(q_1\cos\theta\gamma - \beta E_1)\cos\theta_t - pq_1\sin\theta\cos\varphi\sin\theta_t\}.$$

Thus, neglecting various multiplicative kinematic factors,

$$(\text{New})_1 = (\pi N)_{\text{helicity-conserving}} + \frac{2\mathcal{B}E}{m_p}(E_1\gamma - \beta q_1\cos\theta)$$

and

$$\frac{(\text{New})_1}{(\pi N)_{\text{h.c.}}} = 1 + \theta\left(\frac{1}{s}\right).$$

In this case the s comes explicitly from $\cos\theta_t$ and $\sin\theta_t$; i.e., it is not necessary to use the approximation that $s_{\pi N}$ grows like s to obtain this result. Hence at high energies the large amplitude in our calculation depends only on the πN helicity-conserving amplitude. Thus, the difficulties in matching phase shift and Regge models for the other amplitude do not seriously affect the major results at large energies.

E. The Stodolsky Cancellation in Our Amplitudes

In Sec. III we sketched the argument given by Stodolsky for $L=0$, $M=0$ dominance in a simplified amplitude of form $s_{\pi N}/(t_R - m_\pi^2)$. As the large amplitude in our calculations actually has the form (5.25), multiplied by the pion pole, we now examine this explicitly to see whether an analogous argument still holds.

Since $\mathcal{A}$ and $\mathcal{B}$ are functions of $s_{\pi N}$, with φ dependence only in the form $\sin\theta\cos\varphi\sin\theta_t$, and since $\sin\theta_t$ vanishes in the forward direction of s-channel scattering, we may, to some approximation, assume that $\mathcal{A}$ and $\mathcal{B}$ have no φ dependence. In this approximation the first two terms of (5.25) may be thought of as $M=0$ terms, and the last term as $M=1$. Let us examine them separately.

The pion propagator contains $t_R - m_\pi{}^2$ which may be expressed as

$$t_R - m_\pi{}^2 = \frac{1}{W}[t(W - E_1) - E_1(W^2 - m_\pi{}^2) + \tau_{\pi,3\pi} q_1 \cos\theta] .$$

Hence the $M=0$ term (at large s) is proportional to

$$\frac{\mathcal{B}[q_1\cos\theta(t + W^2 - m_\pi{}^2) - \tau_{\pi,3\pi}E_1]}{t(W - E_1) - E_1(W^2 - m_\pi{}^2) + \tau_{\pi,3\pi} q_1\cos\theta} .$$

Near $t=0$, $\tau_{\pi,3\pi} \approx W^2 - m_\pi{}^2$ and we get

$$\frac{\mathcal{B}(q_1\cos\theta - E_1)}{(q_1\cos\theta - E_1)} = \mathcal{B} .$$

Thus the tail of large-L values expected from the pion propagator will occur only in the lower-order terms from $\mathcal{A}$ although the explicit $\cos\theta$ dependence of $\mathcal{B}$ and of $d^s_{0\lambda}(\psi)$ will introduce some terms with $L \neq 0$.

The $M=1$ amplitude will look like

$$\frac{q_1\sin\theta\cos\varphi}{t_R - m_\pi{}^2} \underset{t\to 0}{\approx} \frac{\sin\theta\cos\varphi}{k - \cos\theta} \propto \cos\varphi(k^2 - 1) \times \sum_{J=1}^{\infty} (2J+1)\left(\frac{J+1}{J}\right)^{1/2} \times Q^{(1,1)}_{J-1}(k) d^J_{10}(\theta) .$$

Hence we expect a long tail of large-L contributions from this piece.

VI. COMMENTS

The simple form of the Deck model allowed us to perform the partial-wave analysis in a relatively straightforward fashion even though all the complications of πN scattering (spin and resonance contributions) were kept. At the heart of this simplification is our treatment of the Reggeized pion exchange, assuming that it couples like an elementary pion. This assumption does the following.

(1) It ensures that all φ_1 dependence of the diagram is in the πN scattering amplitude. This makes the combinations of amplitudes which are even and odd in φ_1 be sums and differences of pairs differing only in the change of sign of the *nucleon* helicities. We found this simplified both calculation and analysis of the results.

(2) It leads to the knowledge that only natural-parity exchange couples at the NN vertex. Higher-spin particles on the exchanged π trajectory could couple with the produced π to form an unnatural-parity state. Our neglect of this allows us to put in on-shell πN scattering.

(3) It allows us to avoid the sort of parameters that would come in if we attempted a form-factor-type continuation of the couplings off shell.

Although we have not stressed agreement with the data in this paper, the calculations presented here do yield magnitudes and relative phases for the partial waves in substantial agreement with the data. Comparison with the data is presented in Ref. 4, after the diagram with $\pi^-\pi^-$ scattering has been added. Presumably a relaxation of our assumption about the pion couplings would allow introduction of some parameters which could be adjusted to attempt to improve agreement with the data.

Having an explicit amplitude with calculable partial waves and phases allowed us to test the fitting program used on 3π data. In general, FIT passed this test very well, despite the complete dissimilarity in form between the Deck model and the cascade decay assumed in the parametrization of FIT. However, we found (a) a systematic problem in estimating relative phases of states containing the $\pi\pi$ $S=0$ wave, and (b) FIT seems to produce a more rounded A_1 peak than does explicit calculation.

APPENDIX

We give here a proof of the "theorem" used in Sec. V B.

Suppose only exchanges of one naturality $\sigma = P_{\rm ex}(-1)^{J_{\rm ex}}$ are present in the t channel of the reaction $\bar{3} + 4 \to \bar{2} + 1$. From the action of the parity operator

$$P(|J\lambda_3\lambda_4\rangle \pm \eta_3\eta_4(-1)^{-s_3-s_4}|J-\lambda_3-\lambda_4\rangle) = \pm(-1)^J(|J\lambda_3\lambda_4\rangle \pm \eta_3\eta_4(-1)^{-s_3-s_4}|J-\lambda_3-\lambda_4\rangle)$$

we deduce that t-channel partial-wave amplitudes for this σ will obey

$$T^J_{\lambda_1\lambda_2;\lambda_3\lambda_4}(t) = \sigma\eta_3\eta_4(-1)^{-s_3-s_4} T^J_{\lambda_1\lambda_2;-\lambda_3-\lambda_4}(t) . \tag{A1}$$

Defining η by $\eta = \eta_3\eta_4(-1)^{+s_3+s_4-\lambda_3+\lambda_4}$, we may then write

$$f^t_{\lambda_1\lambda_2;\lambda_3\lambda_4} \pm \eta\sigma f^t_{\lambda_1\lambda_2;-\lambda_3-\lambda_4} = \sum (2J+1) T^J_{\lambda_1\lambda_2;\lambda_3\lambda_4}(t)[d^J_{\lambda_3-\lambda_4\lambda_1-\lambda_2}(\theta_t) \pm (-1)^{\lambda_4-\lambda_3} d^J_{-(\lambda_3-\lambda_4)\lambda_1-\lambda_2}(\theta_t)] .$$

From standard expressions for the $d^J_{\alpha\beta}$ functions, we see that

(a) as $\cos\theta_t \to \infty$, $d^J_{m-m'}(\theta_t) \to (-1)^{m'} d^J_{mm'}(\theta_t)$;

(b) the combinations $d^J_{mm'}(\theta_t) \pm (-1)^{m'} d^J_{m-m'}(\theta_t)$ have opposite parity under $\theta_t \to \pi - \theta_t$, i.e., $\cos\theta_t \to -\cos\theta_t$;

hence if expanded as series in $\cos\theta_t$, one is composed of odd powers and the other of even powers;

(c) $d^J_{m0} \pm (-1)^m d^J_{-m0} = \begin{cases} 2d^J_{m0}; \\ 0 \end{cases}$

(d) $d^J_{0m} \pm d^J_{0m} = \begin{cases} 2d^J_{0m}. \\ 0 \end{cases}$

We conclude that as $\cos\theta_t \to \infty$,

$$\frac{d^J_{mm'}(\theta_t) - (-1)^{m'} d^J_{m-m'}(\theta_t)}{d^J_{mm'}(\theta_t) + (-1)^{m'} d^J_{m-m'}(\theta_t)} \propto \frac{mm'}{\cos\theta_t}. \tag{A2}$$

Thus for a Regge-pole exchange, or for a single-particle exchange in the t channel, we have

$$\frac{f^t_{\lambda_1\lambda_2;\lambda_3\lambda_4} - \eta\sigma f^t_{\lambda_1\lambda_2;-\lambda_3-\lambda_4}}{f^t_{\lambda_1\lambda_2;\lambda_3\lambda_4} + \eta\sigma f^t_{\lambda_1\lambda_2;-\lambda_3-\lambda_4}} \propto \frac{(\lambda_1-\lambda_2)(\lambda_3-\lambda_4)}{\cos\theta_t}. \tag{A3}$$

---

*Work supported in part by NSF Grant No. GP 25303.
†Work supported in part by AEC Grant No. AT(11-1)-1195.

[1]Yu. Antipov *et al.*, in *Experimental Meson Spectroscopy—1972,* proceedings of the Third International Conference, Philadelphia, 1972, edited by Kwan-Wu Lai and Arthur H. Rosenfeld (A.I.P., New York, 1972), p. 164; G. Ascoli, *ibid.*, p. 185.
[2]G. Ascoli *et al.*, Phys. Rev. D 7, 669 (1973).
[3]G. Ascoli, in *Proceedings of the XVI International Conference on High Energy Physics, Chicago-Batavia, Ill., 1972,* edited by J. D. Jackson and A. Roberts (NAL, Batavia, Ill., 1973), Vol. 1, p. 3.
[4]G. Ascoli *et al.*, Phys. Rev. D (to be published).
[5]S. D. Protopopescu *et al.*, Phys. Rev. D 7, 1269 (1973).
[6]P. Estabrooks *et al.*, CERN Report No. TH. 1661 (unpublished).
[7]A. Donnachie, R. G. Kirsopp, and C. Lovelace, Phys. Lett. 26B, 161 (1968). We used the CERN Theoretical (1967) phase shifts obtained from a tape kindly provided to us by the Particle Data Group, LRL Berkeley.
[8]V. Barger and R. J. N. Phillips, Phys. Rev. 187, 2210 (1969).
[9]G. Höhler and R. Strauss, Z. Phys. 232, 205 (1970). See also F. J. Gilman *et al.*, Phys. Lett. 31B, 387 (1970).
[10]C. D. Froggatt and G. Ranft, Phys. Rev. Lett. 23, 943 (1969).
[11]G. Ranft, Acta. Phys. Pol. A39, 715 (1971).
[12]L. Stodolsky, Phys. Rev. Lett. 18, 973 (1967).
[13]C. Schmid, Phys. Rev. Lett. 20, 689 (1968); Nuovo Cimento 61A, 289 (1969).
[14]B. Weinstein, G. Ascoli, and L. M. Jones, Phys. Rev. D 8, 2904 (1973).
[15]M. Jacob and G. C. Wick, Ann. Phys. (N.Y.) 7, 404 (1959).
[16]T. L. Trueman and G. C. Wick, Ann. Phys. (N.Y.) 26, 322 (1964).